

# Elemental geochemistry and mineralogy of coals and associated coal mine overburden from Makum coalfield (Northeast India)

Binoy K. Saikia<sup>1</sup> · Ananya Saikia<sup>1</sup> · Rahul Choudhury<sup>1</sup> · Panpan Xie<sup>2</sup> ·  
Jingjing Liu<sup>2</sup> · Tonkeswar Das<sup>1</sup> · Hari P. Dekaboruah<sup>3</sup>

Received: 14 November 2015 / Accepted: 18 February 2016 / Published online: 11 April 2016  
© Springer-Verlag Berlin Heidelberg 2016

**Abstract** The insufficient research on the nature and mode of occurrence of minerals and other inorganic elements of the Northeast Indian coal deposits has resulted in lack of proper utilization, assessment and mitigation of environmental degradation. The mineralogical and geochemical aspects of these coals were studied through the techniques such as optical microscopy, low temperature quantitative X-ray diffraction (LTA-XRD), scanning electron microscopy energy dispersive spectroscopy (SEM-EDS), inductively coupled mass spectroscopy (ICP-MS) and chemical analysis techniques. The leaching behavior of the elements including REEs in presence of water was studied. The high organic sulfur (>75 % of total sulfur) and low ash yields were observed in these coals, varying with seam depth. The dominance of vitrinite (94.1–94.3 %) with an  $R_{\max}$  0.72–0.78 % in these coals along with their dominance within the lean organic fraction in the coal mine overburden (OB) samples was reported. The major oxides present in these coals and their associated overburden samples were studied through XRF analysis. Various mineral phases were identified in both coal and OB samples such as dawsonite, pyrite, diaspore, marcasite, gypsum, thenardite berzeliite (garnet), etc. The SEM-EDS analysis indicated the presence of siderite, pyrite,

and kaolinite, quartz, illite, etc., in the coal, OB and leached samples. The distribution of concentrations of the 48 trace and rare earth elements (REEs) varying with seam depth were normalized by upper continental crust (UCC) and found to be lower in comparison to global, Chinese, and USA coals. The statistical analysis on the trace and rare earth elements in the coals was performed to know their mutual correlations.

**Keywords** Indian coal · Mineralogy of coal · Geochemistry of coal · Coal mine overburden · Rare earth elements · Leaching of coal

## Introduction

There are both academic and industrial interests in studying different properties of coals. The development in the field of petrology, mineralogy, and geochemistry of coal has played a significant role in both the industrial utilization and the broad understanding of environmental degradation due to coal mining activities. India has large coal reserves, about 301.56 Gt (Central Statistics Office 2015), found in both the Permian Gondwana formations of peninsular India and Eocene to Oligocene formations (40–55 million years) from the northeastern region (NER). The coal resources in the NER are about 1500 Mt distributed predominantly in the states of Assam, Meghalaya Nagaland, and Arunachal Pradesh (Central Statistics Office 2015). Although the northeastern region contains meager quantity of mineable coal reserves, the Makum coalfield is one of the country's best coalfields, having good quality coal characterized by very low ash yield, high volatile matter, and high caking index, but with >2.0 % total sulfur (>75 % of the total as organic sulfur). These coals have the characteristics needed for coal liquefaction (Baruah et al. 2013) and can also be a blendable

✉ Binoy K. Saikia  
bksaikia@gmail.com; bksaikia@rrl.jorhat.res.in

<sup>1</sup> Coal Chemistry Division, CSIR-North East Institute of Science and Technology, Jorhat 785006, India

<sup>2</sup> State Key Laboratory of Coal Resources and Safe Mining, China University of Mining and Technology (Beijing), D11, Xueyuan Road, Haidian District, Beijing 100083, People's Republic of China

<sup>3</sup> Bio-Technology Division, CSIR-North East Institute of Science and Technology, Jorhat 785006, India

coal for steel industry if the sulfur is removed. A large amount of work has been carried out on the removal of organic sulfur from NER coals and has been observed to be very difficult (Saikia et al. 2014a, b). The presence of high sulfur contents in these coals creates environmental degradation including acid mine drainage (AMD) around the coalfield (Baruah 2009). Owing to its low inorganic sulfur (<1 %), the environmental impact of coal mining activities in these coalfields is significant (Barooah and Baruah 1996). The extent of AMD is not only affected by the mineralogy and geochemistry of the coals but also by the accompanying strata of the coalfields (Jamal et al. 1991). However, the mineralogical and geochemical aspects of this coalfield are poorly understood and urgently need to be explored.

Therefore, this study attempts to understand the mineralogy, geochemistry, and leaching behavior of elements in NER coals and overburden samples, which may also provide a path for environmental management of the region. The leaching behavior of the elements, including REEs, will provide information on the mobility of metals in the surrounding area of Makum coalfield. Special emphasis has been given on the distribution of the rare earth elements (REEs) in these samples due to their economic importance. Despite their global significance, the distribution of REEs in northeastern coalfields is still poorly known. Furthermore, to the authors' knowledge, there has been no study on the occurrences, distribution, and leaching behavior of REEs in northeastern high-sulfur coals and mine overburdens. The petrographical, mineralogical, geochemical, and elemental studies were carried out for coal and coal mine overburden of Makum coalfield, Assam, India. Thus, this paper attempts to provide a comprehensive database of the distribution of the elements in these important coals of the world, and also to understand the behavior of the major, minor, trace, and rare earth elements during aqueous leaching.

An understanding of the speciation of minerals such as pyrite present in coals and overburden is needed to predict their extent of transformation and mobilization to design the best management technology for AMD. There is a scarcity of information on the nature, precise concentrations, and mode of occurrence of minerals as well as the elemental composition in northeastern coals and overburden. The overall geochemical studies presented in this paper will be effective in designing the mitigation processes for the AMD problem in the region.

## Geological setting of Makum coalfield, Northeast India

The Makum coalfield (latitudes 27°15'–27°25'N and longitudes 95°40'–95°55'E), the most important coalfield of northeast India, is situated along the outermost flank of the

Patkai range. This coalfield, encompassing the Baragolai, Ledo, Namdang, Tikak, Tipong, and Tirap collieries, is composed of detached, isolated tectonic blocks in the Belt of Schuppen (Sarmah 2013). The geographical location and lithostratigraphy of the Makum coalfield are shown in Figs. 1, 2, respectively.

The geological structure of the coalfield is a well-defined asymmetrical northeast plunging syncline with a closure at the Namdang colliery, known as Namdang syncline. The sedimentary rocks were folded and thrust under the impact of several orogenic movements. The coal basin is demarcated by the Margherita thrust on the north and the Halfong-Disang thrust on the south. A number of sympathetic faults have originated due to the effect of both thrust faults. These faults are either parallel or sub-parallel to the trends of the major thrust. The alignments of the major thrusts have not been properly delineated; particularly the Margherita thrust which is beneath a thick alluvium and vegetation cover (GSI 2009).

The coal beds of Makum coalfield occur in the Oligocene Tikak Parbat Formation of Barail Group comprising of alternations of sandstone, siltstone, mudstone, carbonaceous shale, clay, and coal seams. The Tikak Parbat Formation (18-m thickness) is underlain by predominantly massive, micaceous or ferruginous sandstones that comprise the Baragolai Formation, which in turn is underlain by thin-bedded, fine-grained quartzitic sandstones with thin shale and sandy shale partings that make up the Naogaon Formation (GSI 2009). Together, the three formations comprise the Barail Group. The coal bearing Tikak Parbat Formation on the southern limb of the Namdang syncline abuts against the Haflong Disang Thrust and reappears again in the east near Lekhapani mine entry (GSI 2009). The coal bearing formation continues in the east. This formation has five coal seams out of which only the 20 and 60 feet are workable (GSI 2009).

## Methodology

### Collection of samples

The Tirap open cast coal mine is the most active and industrially important coal mine in the Makum coalfield (Northeast India). The 6 and 18 m are the two workable seams of the Tikak Parbat and Baragolai Formations of the Barail Group of the coalfield. Bulk coal samples (T-20F, T-60F, T2-60F and MK-60F) from run-of-mine (ROM) of the 6 and 18 m seams of Tirap coal mine in Makum coalfield were collected by using standard method (ASTM 2011a). By adopting same method, three coal mine overburden (OB) samples (TO-20F, TO-60F and LS-60F), dominantly sandstones and shales, were also collected from the overburden dumps associated with the above coal seams.

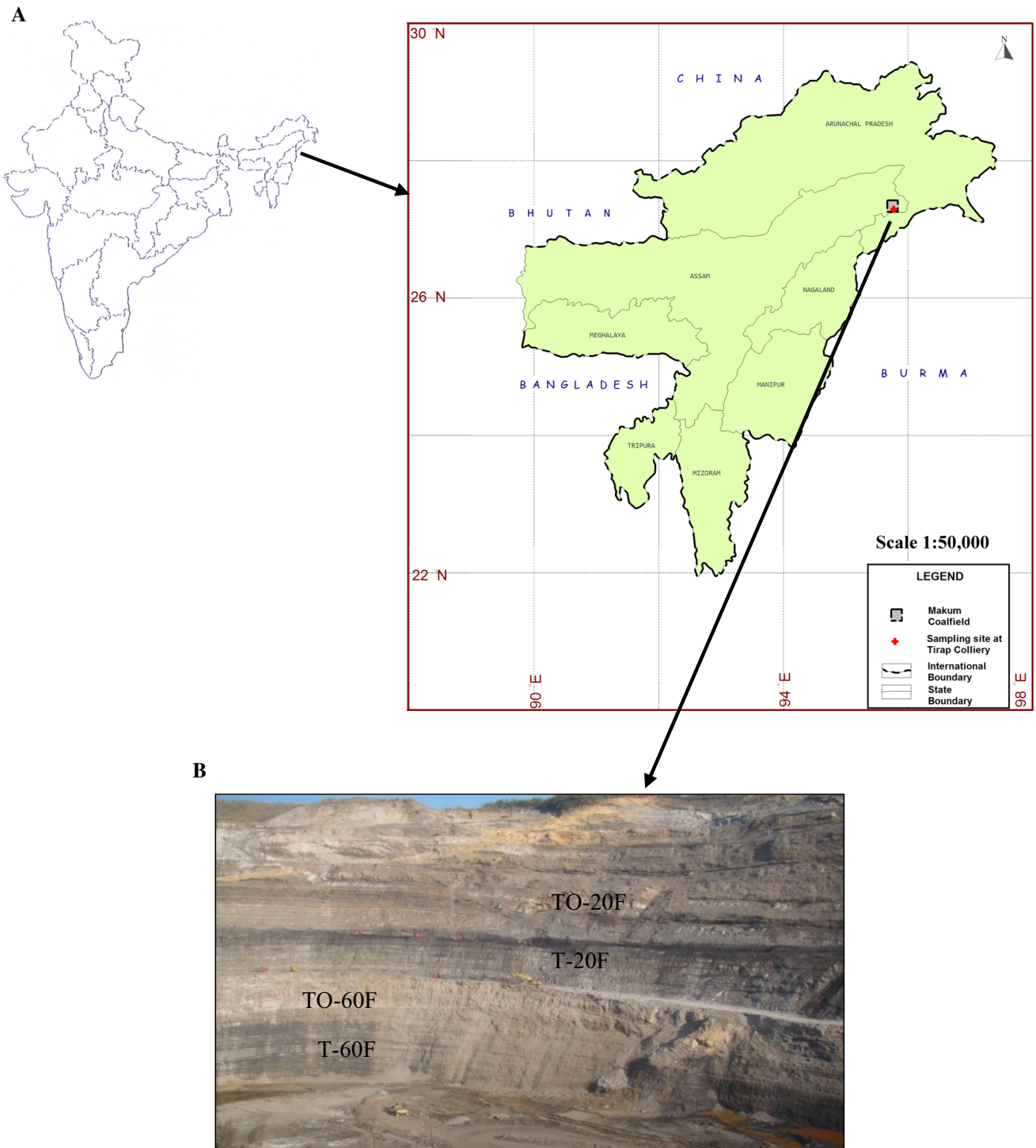


**Fig. 1** a Map showing the area of Makum coalfield (Northeast India). b Photograph of the studied coal seams and overburden

**Chemical analysis**

The coal and mine overburden samples were analyzed to determine their chemical properties. Proximate analysis of the coal samples were done by using a thermogravimetric analyser (Model: TGA 701; Leco Corporation, USA)

according to ASTM standard method (ASTM 2011b, c, d). The contents of carbon, hydrogen, and nitrogen were determined using a Perkin-Elmer 2400 Elemental Analyser; total sulfur was determined by a ‘Sulfur Analyser’ (Model: S-144DR; Leco Corporation, USA) following standard methods (ASTM 1991, 2002). The forms of sulfur

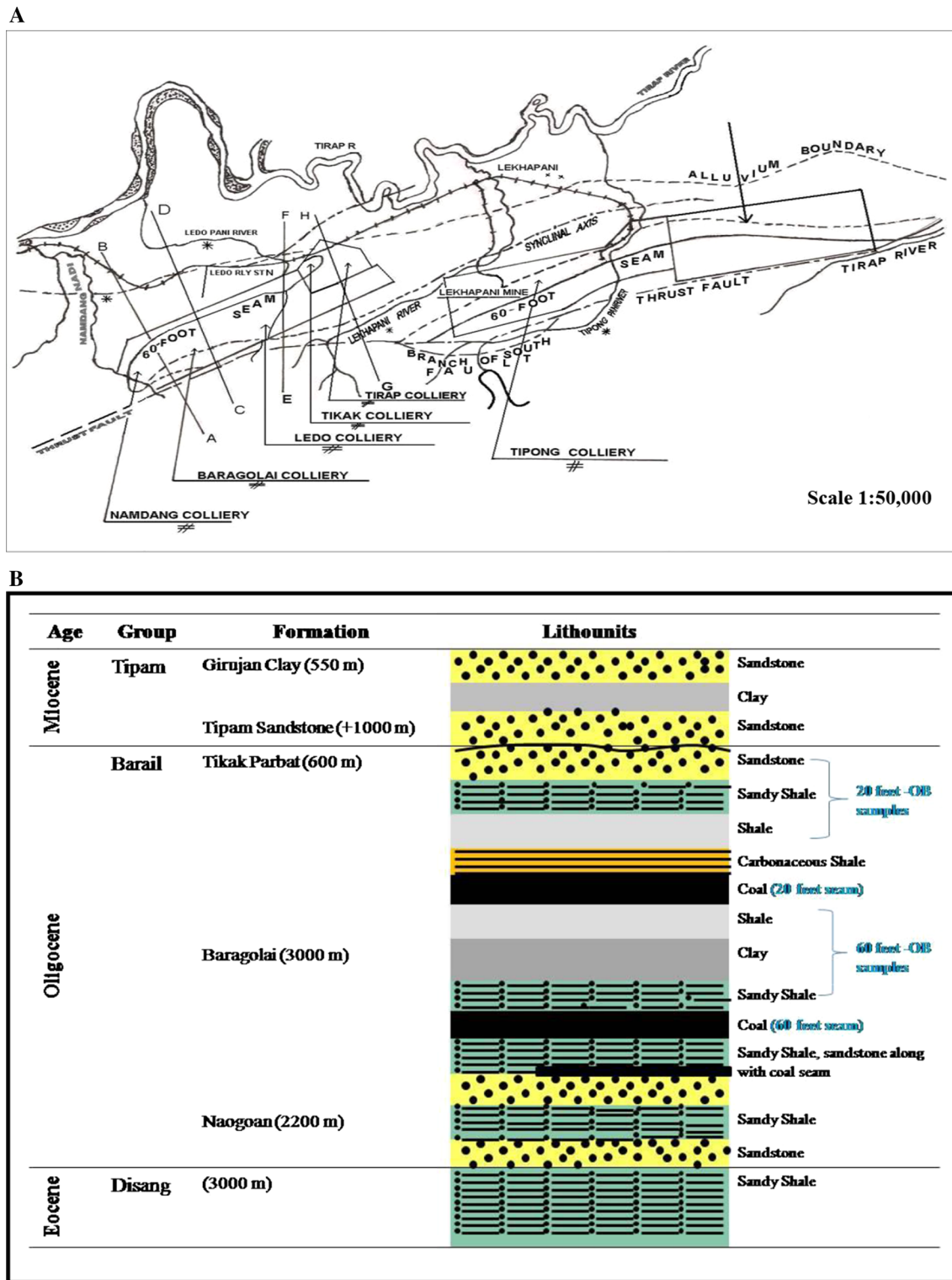


Fig. 2 a Geological map and b lithostratigraphy of Makum coalfield (Northeast India)

in the coal samples (pyritic and sulfate sulfur) were determined following the ASTM standard method (ASTM 2005), and the percentages of organic sulfur calculated by the difference from total sulfur.

### Petrography

Samples of each coal and overburden were prepared as epoxy-bound particulate pellets, and finished with a final

0.05- $\mu\text{m}$ -alumina polish. The samples were examined by reflected light microscopy under a Leitz Orthoplan microscope, using a 50- $\times$  oil-immersion objective, to provide petrographic information, especially of the organic matter. Description of the coal and overburden samples followed ICCP (1998, 2001) nomenclature for vitrinite and inertinite and Taylor et al. (1998) for liptinite. Vitrinite reflectance measurement followed the appropriate ASTM standard (ASTM 2011e).

### Mineral characterization

#### *XRD analysis*

The mineralogy was determined by optical microscopic observation and X-ray powder diffraction (XRD). Low-temperature ashing (LTA) of coal was performed using an EMITECH K1050X plasma asher prior to XRD analysis. XRD analysis of the low-temperature ashes was performed on a powder diffractometer (D/max-2500/PC XRD) with Ni-filtered Cu-K $\alpha$  radiation and a scintillation detector. The XRD pattern was recorded over a  $2\theta$  interval of  $2.6^\circ$ – $70^\circ$ , with a step size of  $0.01^\circ$ . X-ray diffractograms of the LTA samples were subjected to quantitative mineralogical analysis using Siroquant<sup>TM</sup>, commercial interpretation software developed by Taylor (1991) based on the principles for diffractogram profiling set out by Rietveld (1969). Further details indicating the use of this technique for coal-related materials are given by Ward et al. (1999, 2001), Ruan and Ward (2002), and Dai et al. (2012a, b).

#### *SEM–EDS analysis*

A field emission scanning electron microscope (FE-SEM, FEI Quanta<sup>TM</sup> 650 FEG), in conjunction with an EDX energy-dispersive X-ray spectrometer (Genesis Apex 4) was used to study the morphology of the minerals and also to determine the distribution of some elements (Dai et al. 2012a, b). Samples were carbon coated using a Quorum Q150T ES sputtering coater. Samples were mounted on standard aluminum SEM stubs using sticky electronic conductive carbon tabs. The working distance of the FE-SEM–EDS was 10 mm, the beam voltage was 20.0 kV, the aperture was 6, and the spot size was 5  $\mu\text{m}$ . The images were captured via a retractable solid state backscatter electron detector.

### Chemical characterization

#### *XRF analysis*

A separate representative portion of each coal and OB sample was ashed at  $815^\circ\text{C}$ . The (high temperature) ashes

of the two coals, and also the overburden and fly ash samples (without ashing), were calcined at  $1050^\circ\text{C}$ , fused with lithium metaborate and cast into discs, following the method of Norrish and Hutton (1969). The discs were analyzed by X-ray fluorescence (XRF) spectrometry using a Philips PW 2400 spectrometer and *SuperQ* software, and the results expressed as percentages of the major element oxides in each sample. The loss on ignition at  $1050^\circ\text{C}$  for each overburden and fly ash sample was also determined as part of the analysis process.

#### *Trace elements analysis*

Inductively coupled plasma mass spectrometry (ICP-MS) was used to determine the most trace elements in the coal and OB samples, following the techniques outlined by Dai et al. (2011). Prior to ICP-MS analysis, the samples were digested using an UltraClave Microwave High Pressure Reactor. The digestion reagents for each 50-mg coal sample are 5-ml 65 %  $\text{HNO}_3$  and 2-ml 40 % HF. Arsenic and Se were determined by ICP-MS, using collision cell technology (CCT) to avoid disturbance of polyatomic ions (Li et al. 2014). The Guaranteed Reagent  $\text{HNO}_3$  and HF for sample digestion were further purified by sub-boiling distillation. Standard references of Inorganic Ventures (CCS-1, CCS-4, CCS-5, and CCS-6), NIST 2685b, and Chinese standard reference GBW 07114) were used for the calibration of trace element concentrations obtained by ICP-MS.

### Aqueous leaching experiment of coal and OB samples

An aqueous static leaching experiment was carried out in the laboratory by taking 50 g of the coal (T-20F and T-60F) and OB (TO-20F and TO-60F) samples and adding 250 mL of deionized water in a 1-L conical flask at atmospheric conditions. The mixture was stirred for a period of 8 h and filtered. The elemental concentrations in the aqueous leachates as well as the washed coal residues were determined by using ICP-MS methods. The mineralogy of the washed coal samples were also examined by SEM–EDS technique.

### Statistical analyses of the elements

The statistical tests such as significant tests, bivariate analysis and principal component analysis (PCA) were applied to the concentrations of the trace elements and REE in the raw and leached coal, raw and leached OB, and water leachate samples with the aid of SPSS16 software.

**Table 1** Physico-chemical characteristics of coal and overburden samples (as received basis; wt%)

| Samples | M    | A     | VM    | FC    | S <sub>t</sub> | S <sub>py</sub> | S <sub>sulp</sub> | S <sub>org</sub> | C     | H    | N    | O    |
|---------|------|-------|-------|-------|----------------|-----------------|-------------------|------------------|-------|------|------|------|
| T-20F   | 2.09 | 1.90  | 41.25 | 54.76 | 1.90           | 0.38            | 0.18              | 1.34             | 82.70 | 6.01 | 1.0  | 4.4  |
| T-60F   | 1.75 | 2.95  | 41.19 | 54.11 | 3.62           | 0.46            | 0.21              | 2.95             | 82.10 | 5.98 | 1.1  | 2.5  |
| T2-60F  | 1.80 | 2.50  | 43.80 | 51.90 | 3.45           | 0.52            | 0.22              | 2.71             | 81.40 | 5.64 | 1.10 | 4.41 |
| MK-60F  | 2.99 | 4.11  | 42.5  | 50.30 | 3.76           | 0.48            | 0.25              | 3.03             | 83.1  | 6.47 | 1.00 | 1.47 |
| TO-20F  | 1.52 | 82.00 | 15.62 | 0.85  | 3.16           | 0.39            | 0.24              | 2.53             | 6.05  | 1.28 | nd   | nd   |
| TO-60F  | 1.41 | 82.01 | 15.86 | 0.72  | 2.82           | 0.52            | 0.34              | 1.96             | 4.02  | 1.03 | nd   | nd   |
| LS-60F  | 2.41 | 77.84 | 17.38 | 2.37  | 4.22           | 0.26            | 0.57              | 3.39             | 9.61  | 1.00 | nd   | nd   |

M moisture, VM volatile matter, FC fixed carbon, S<sub>t</sub> total sulfur, S<sub>py</sub> pyritic sulfur, S<sub>sulp</sub> sulfate sulfur; S<sub>org</sub> organic sulfur, C carbon, H hydrogen, N nitrogen, nd not determined

## Results and discussion

### Chemical characteristics of coal and OB samples

The summary of the chemical properties of the coal and OB samples are shown in Table 1. The coals as well as the OB samples are medium to high sulfur in nature with high organic sulfur contents (>75 % of the total S) (Chou 2012). The carbon and hydrogen contents of the coals fall in the range of 81.40–83.10 % and 5.64–6.47 %, respectively, whereas in cases of OB samples, the carbon and hydrogen contents are found to be 4.02–9.61 % and 1.00–1.28 %, respectively, on as received basis. There are variations of the chemical properties with respect to their seam depth from 6 to 18 m, as summarized in Table 1.

### Petrography of the coal and OB samples

The high volatile A bituminous T-20 and T-60 coals, with an  $R_{\max}$  0.72–0.78 %, are dominated by vitrinite (94.1–94.3 %), with collotelinite (73.7–77.2 %) being the most abundant maceral subgroup within the vitrinite group followed by vitrodetrinite (13.6–15.3 %) and telinite (2.8–4.9 %) (Table 2). The vitrinite macerals of the studied coal samples are more in comparison to that of other Indian coals, e.g., Jharia coalfield, Jharkhand (vitrinite 32.04–74.90 % with  $R_{\max}$  1.23–2.03 %) (Karmakar et al. 2013) and Ib valley coalfield, Orissa (vitrinite 4.5–80.2 %) (Senapaty and Behera 2015). The  $R_{\max}$  is an important coal rank parameter and helps in measuring accurately minor differences in coal used for coke making. The  $R_{\text{random}}$  of T-20 and T-60 is 0.66–0.69 %. As the  $R_{\text{random}} < 0.90$  %, the difference between  $R_{\max}$  and  $R_r$  values becomes insignificant, and thus,  $R_{\max}$  study is considered to be useful for the present study (Komorek and Rafał 2002). The coal fractions of the OB samples are dominantly composed of vitrinite macerals. Vitrinite group macerals are even more dominant within the lean organic fraction in the TO samples. Trace amounts of funginite and liptinite macerals

were observed in the TO samples (Table 2; Fig. 3). Lesser amounts of inertinite (2.6–3.9 %) and liptinite (1.8–3.3 %) are also found in the coal samples in comparison to other Indian coals such as Jharia (inertinite 15.02–51.40 %, liptinite 0.02–10.40 %) (Karmakar et al. 2013) and Ib valley coalfield, Orissa (inertinite 12.5–92.2 %, liptinite 3.30–22.2 %) (Senapaty and Behera 2015). The large vitrinite fragment of Fig. 3a is a reworked vitrinite fragment showing relief and rounded margins, and it is deposited in an epoxy matrix. Tiny pyrites are also present. The fragment seems to be transported and possibly this may be the reason for the compressed form of the funginites.

The abundance of vitrinite in the studied coal samples indicates that the coal originated in a wet forest swamp mainly from arborescent vegetation (Suwarna 2006; Suárez-Ruiz and Ward 2008; Solaymani and Taghipour 2012). Other coals of Makum coalfield show varying proportions of vitrinite (92.7–65.5 %), liptinite (22.0–0.6 %), and inertinite along with mineral matter and shale or clay, and were deposited under the influence of marine environment (Baruah et al. 2013).

A coal facies diagram based on two petrographic parameters: the tissue preservation index (TPI) and the gelification index (GI), has been developed to represent the palaeoenvironmental conditions during peat accumulation (Diessel 2012). The index of coal facies analysis is:

$$GI = (\text{Vitrinite} + \text{Macrinite}) / (\text{Fusinite} + \text{Semifusinite} + \text{Inertodetrinite})$$

$$TPI = (\text{Telinite} + \text{Collotelinite} + \text{Semifusinite} + \text{Fusinite}) / (\text{Collodetrinite} + \text{Macrinite} + \text{Inertonertinite} + \text{Vitrodetrinite} + \text{Corpogelinite})$$

The GI and TPI indexes for 20 feet coal seam are 157 and 5.65, whereas for 60 feet are 94.7 and 4.94. The high GI and TPI values indicates clastic marsh to forest swamp of limno-telmatic condition which is the typical characteristics of lower delta plain environment prevailed under wet (peat) land set-up and the high TPI value is due to high

**Table 2** Macerals in coal and overburden samples (vol %), plus maximum and random vitrinite reflectances ( $R_{max}$  and  $R_r$ , %) and V-types (% distribution of vitrinite maximum reflectance in 0.1 % increments)

| Macerals             | T-20F |                    | T-60F |                    | TO-20F |                    | TO-60F |                    |
|----------------------|-------|--------------------|-------|--------------------|--------|--------------------|--------|--------------------|
|                      | Total | Mineral-free basis | Total | Mineral-free basis | Total  | Mineral-free basis | Total  | Mineral-free basis |
| Telinite             | 2.8   | 2.8                | 4.8   | 4.9                | 0.5    | 6.7                | 0.5    | 11.1               |
| Collotelinite        | 76.5  | 77.2               | 72.4  | 73.7               | 5.5    | 73.3               | 4.0    | 88.9               |
| Total telovitrinite  | 79.2  | 80.1               | 77.2  | 78.6               | 6.0    | 80.0               | 4.5    | 100.0              |
| Vitrodetrinite       | 13.4  | 13.6               | 15.0  | 15.3               | 1.5    | 20.0               | 0.0    | 0.0                |
| Collodetrinite       | 0.0   | 0.0                | 0.0   | 0.0                | 0.0    | 0.0                | 0.0    | 0.0                |
| Total detrovitrinite | 13.4  | 13.6               | 15.0  | 15.3               | 1.5    | 20.0               | 0.0    | 0.0                |
| Corpogelinite        | 0.3   | 0.3                | 0.4   | 0.4                | 0.0    | 0.0                | 0.0    | 0.0                |
| Gelinite             | 0.3   | 0.3                | 0.0   | 0.0                | 0.0    | 0.0                | 0.0    | 0.0                |
| Total gelovitrinite  | 0.5   | 0.5                | 0.4   | 0.4                | 0.0    | 0.0                | 0.0    | 0.0                |
| Total vitrinite      | 93.2  | 94.1               | 92.6  | 94.3               | 7.5    | 100.0              | 4.5    | 100.0              |
| fusinite             | 0.3   | 0.3                | 1.0   | 1.0                | 0.0    | 0.0                | 0.0    | 0.0                |
| Semifusinite         | 0.0   | 0.0                | 0.0   | 0.0                | 0.0    | 0.0                | 0.0    | 0.0                |
| Micrinite            | 0.0   | 0.0                | 0.0   | 0.0                | 0.0    | 0.0                | 0.0    | 0.0                |
| Macrinite            | 0.0   | 0.0                | 0.4   | 0.4                | 0.0    | 0.0                | 0.0    | 0.0                |
| Secretinite          | 0.5   | 0.5                | 0.0   | 0.0                | 0.0    | 0.0                | 0.0    | 0.0                |
| Funginite            | 1.5   | 1.5                | 2.4   | 2.4                | 0.0    | 0.0                | 0.0    | 0.0                |
| Inertodetrinite      | 0.3   | 0.3                | 0.0   | 0.0                | 0.0    | 0.0                | 0.0    | 0.0                |
| Total inertinite     | 2.5   | 2.6                | 3.8   | 3.9                | 0.0    | 0.0                | 0.0    | 0.0                |
| Sporinite            | 1.5   | 1.5                | 0.4   | 0.4                | 0.0    | 0.0                | 0.0    | 0.0                |
| Cutinite             | 0.0   | 0.0                | 0.0   | 0.0                | 0.0    | 0.0                | 0.0    | 0.0                |
| Resinite             | 1.0   | 1.0                | 1.0   | 1.0                | 0.0    | 0.0                | 0.0    | 0.0                |
| Alginite             | 0.0   | 0.0                | 0.0   | 0.0                | 0.0    | 0.0                | 0.0    | 0.0                |
| Liptodetrinite       | 0.8   | 0.8                | 0.2   | 0.2                | 0.0    | 0.0                | 0.0    | 0.0                |
| Suberinite           | 0.0   | 0.0                | 0.0   | 0.0                | 0.0    | 0.0                | 0.0    | 0.0                |
| Exsudatinite         | 0.0   | 0.0                | 0.2   | 0.2                | 0.0    | 0.0                | 0.0    | 0.0                |
| Total liptinite      | 3.3   | 3.3                | 1.8   | 1.8                | 0.0    | 0.0                | 0.0    | 0.0                |
| Silicate             | 1.0   |                    | 1.0   |                    | 89.0   |                    | 89.1   |                    |
| Sulfide              | 0.0   |                    | 0.8   |                    | 3.5    |                    | 5.0    |                    |
| Carbonate            | 0.0   |                    | 0.0   |                    | 0.0    |                    | 1.5    |                    |
| Other                | 0.0   |                    | 0.0   |                    | 0.0    |                    | 0.0    |                    |
| Total mineral        | 1.0   |                    | 1.8   |                    | 92.5   |                    | 95.5   |                    |
| $R_{max}$            | 0.78  |                    | 0.72  |                    |        |                    |        |                    |
| St dev               | 0.03  |                    | 0.03  |                    |        |                    |        |                    |
| $R_{random}$         | 0.66  |                    | 0.69  |                    |        |                    |        |                    |
| St dev               | 0.03  |                    | 0.02  |                    |        |                    |        |                    |

content of structural vitrinite group (Potter et al. 2008). However, the majority of other Indian coals were deposited under conditions intermediate to dry forest and wet forest swamps (Mishra et al. 2005).

**XRD data**

Quartz and Kaoline are dominant in majority of the Indian coals along with calcite, pyrite, illite and anatase. Siderite

is mainly associated with the vitrinite macerals (Nath et al. 2005)

The proportion of each crystalline phase identified from X-ray diffractograms of the coal and overburden samples is shown in Table 3. Kaolinite is the dominant mineral in all the coal and OB samples except in 18 m OB samples followed by quartz. The XRD data of the two Paleogene coals and their associated mine overburden show the dominance of minerals (with >10 %) such as kaolinite,

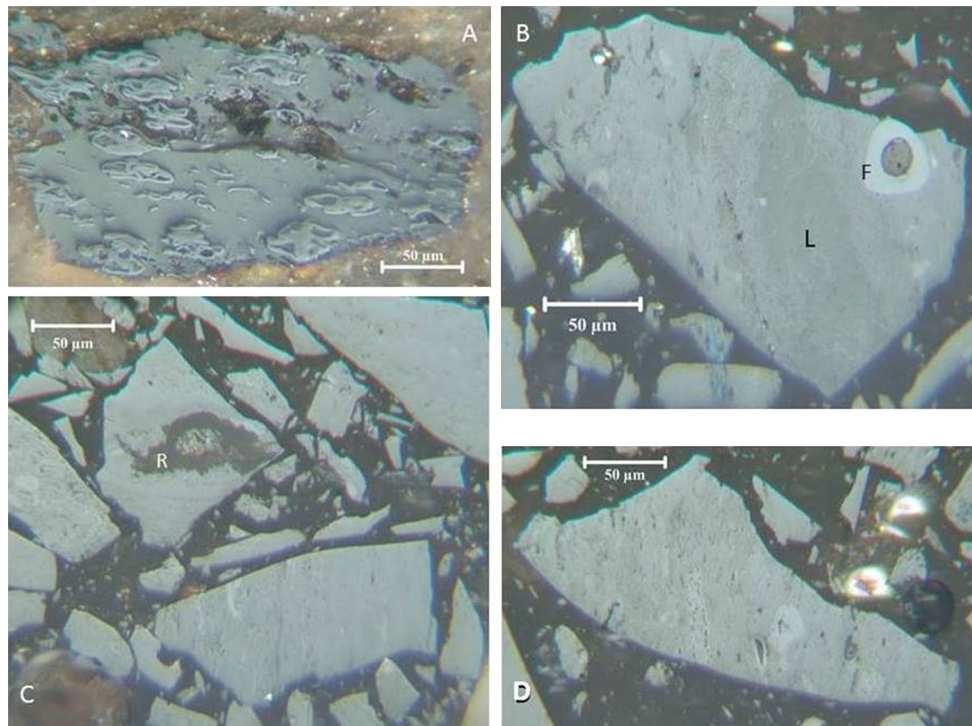


**Fig. 3** **a** Compressed funginite in collotelinite matrix (TO-20F sample); **b** faint liptinite (collotelinite B) (L) with vitrinite macerals and funginite (F). (TO-60F); **c** funginite in resinite (R). (TO-20F); **d** funginite in detrovitrinite matrix. (TO-20F)

dawsonite, quartz, and illite in coal as well as the OB samples. Pyrite present in these coals occurs as tiny grains in vitrinite and increases in abundance towards the younger seams (Saikia et al. 2014a, b). Calcite and lenses of clay minerals are also recognized as impregnations and thin layers, respectively, in vitrinite macerals in these coals (Saikia et al. 2014a, b). However, mineralogy of the coals is observed to be significantly different between the 6 and 18 m coal seams. Diaspore, albite, and berzeliite present in T-20F coals are not observed in T-60F coal sample. The occurrence of albite in the coal samples is likely to be of hydrothermal origin, indicating a possible relation to submarine exhalation (Dai et al. 2008). Dawsonite in coal usually forms in hydrothermal environments (Dai et al. 2008). In these Paleogene coals, it is probably formed by the thermal decomposition of aluminous silicates minerals (Loughnan and Goldbery 1972), which are significantly high in northeast Indian coals. Dawsonite also may be formed due to alteration of K-feldspar and plagioclase minerals present in the samples (Loughnan and Goldbery 1972). Berzeliite, from garnet structural group, is observed in T-20F coal sample, and is reported for the first time in any Indian Paleogene coals.

The kaolinite content in these coals ranges from 26.7 to 34.7 %. The kaolinite minerals may have formed in coal bearing and overburden areas due to movement of leachates in high pH areas, causing interaction of the

precipitated alumina with the silica-rich solutions (Ward 2002). The presence of pyrite in these coal and OB samples may be due to the transformation of Fe-bearing minerals to pyrite by the reaction with dissolved sulfides or polysulfides, which also support the marine influence on these

**Table 3** XRD analysis of minerals in the coal and OB ash samples (wt%)

| Phase              | T-20F      | T-60F | TO-20F | TO-60F |
|--------------------|------------|-------|--------|--------|
|                    | Weight (%) |       |        |        |
| Kaolinite          | 41.1       | 34.7  | 37.7   | 26.7   |
| Dawsonite          | 29.3       | 15.9  | –      | –      |
| Quartz             | 14.3       | 22.4  | 37     | 40.9   |
| Dolomite           | 5.5        | 4     | –      | –      |
| Illite             | 4.6        | 7.2   | 12.7   | 13.3   |
| Diaspore           | 1.7        | –     | –      | –      |
| Albite (low)       | 1.4        | –     | –      | –      |
| Pyrite             | 1.3        | 5.8   | 4.7    | 4.4    |
| Berzeliite, garnet | 0.4        | –     | –      | –      |
| Calcite 2          | 0.3        | 0.6   | –      | –      |
| Marcasite          | –          | 7.8   | –      | –      |
| Rutile             | –          | 1.5   | 0.2    | –      |
| Gypsum             | –          | –     | 6.2    | 8.6    |
| Thenardite         | –          | –     | 1.4    | 5.6    |
| Anatase            | –          | –     | 0.1    | 0.5    |



Paleogene coals of Makum coalfield (Chou 2012; Nayak 2013).

Similar type of mineralogy is observed for the associated OB samples except for the presence of thenardite in the OB samples (Table 3). Thenardite from mine overburden may easily dissolve in water to produce sulphuric acid, causing acid mine drainage in these coal mines. Thus, although these Paleogene coals have low pyritic sulfur, they produce a large amount of acid mine drainage which may be due to the other sulfur minerals in coal and associated overburden. The OB samples contain gypsum (calcium sulfate) and thenardite (sodium sulfide). These minerals may have been deposited within the OB samples by generation of gases escaping from the surficial fractures and veins of the OB rocks during the contact of rainwater with the overburden heap (Masalehdani et al. 2009). The gypsum may, however, also be a precipitation product derived from Ca and SO<sub>4</sub> in the pore waters of the OB samples with drying (Ward 2002).

### Observation from SEM–EDS

SEM–EDS examination also reveals the presence of siderite, pyrite, and kaolinite in the 18 m coal and leached coal samples (Fig. 4). The occurrence of pyrite in both the coal (as agglomerate in shape) and leached coal samples (as elongate in shape) indicate that the coal seams were formed under the influence of marine conditions (Chou 2012; Dai et al. 2013). The presence of kaolinite in the studied 18 m samples indicates that the samples are enriched in aluminosilicates and in REEs. Siderite could not be identified by XRD analysis, which is due to the fact that the lattice of siderite collapses at ~500 °C that is far higher temperature than of the LTA.

On the other hand, the 18 m OB and leached OB samples contain pyrite, quartz, kaolinite, illite, Fe-magnesite, mixed-layer illite/smectite, and Ti-oxide (antase) (Fig. 5). The pyrite occurs in different forms in the studied OB samples which ranges from agglomerated framboidals, quadrilateral to triangular in shapes. The pyrite found in the other coalfields of NE region such as Jaintia Hills, Meghalaya occurs as framboid, colloidal precipitate, colloform-banded, fine disseminations, discrete grains, dendritic (feathery), recrystallized, nuggets, discoidal, massive, cavity-fracture- and cleat-fillings (Nayak 2013).

The high concentration of clay minerals (kaolinite, illite, and mixed-layer illite/smectite) in the OB samples suggests that during peat accumulation, detrital sediments were mixed with the allochthonous organic debris (as stated in the nature of vegetation in the petrographical study), but later these sediments were excluded after the swamp had become more fully established. The distribution of clay minerals in the OB samples may be due to the alteration of

detrital sediments when the peat forming conditions were dominant (Ward 2002). The presence of quartz in the OB samples suggests their derivation from the basement rocks or from siliceous phytoliths within the peat-forming plant tissues (Ward 2002).

### XRF data

The chemical composition of the high-temperature (815 °C) ash for the coal and OB samples is given in Table 4. The XRF analysis of the major oxides reveals the presence of high portions of Al<sub>2</sub>O<sub>3</sub>, SiO<sub>2</sub>, and Fe<sub>2</sub>O<sub>3</sub> in both Paleogene coals and their associated overburden samples. These three oxides together make up 75–94 % of the chemical compositions of the ashes. The higher percentages of SiO<sub>2</sub> and Al<sub>2</sub>O<sub>3</sub> indicate the dominance of the aluminosilicate minerals in the coal and OB samples. However, other major significant oxides are also observed in the samples as shown in Table 4. There are notable variations in the concentrations of the major oxides in the coals as well as OB samples with respect to their seam depth.

### Elemental composition of the coal and OB samples

The Indian coals show decreasing concentration of the volatile elements (Ge, Ga, Cd, Sb, Sn, Pb, etc.) with higher concentrations of V, Cr, Mn, Zn, Na, K, etc. (Banerjee et al. 2002). The concentrations of the 48 trace elements along with the REE present in the coal and the OB samples are listed in Table 5. Variations in the concentrations of the trace elements with depth can be seen for both coal (T-20F, T-60F, T2-60F and MK-60F) and OB samples (TO-20F, TO-60F). Some of the elements show a large difference in their concentrations between the 6 to 18 m coal seams.

Out of the 48 trace elements, the most abundant trace elements observed in these Paleogene coals are Sr, Zr, Ba, Cr, Li, V, Zn, and, to a lesser extent, Cu and Pb. Lower concentrations of Be, Sc, Ge, Rb, In, Cs, Hf, Ta, W, Bi and Th are also observed in the coal and OB samples. Moreover, in two of the coal samples (T2-20F and MK-60F), the concentrations of Se, Sb, and U are abundant. The lowering of the concentrations of calcite from T-20F to T-60F coal (Table 5) coincides with the decrease in the concentration of Sr from 190 to 2.65 ppm in the respective coal samples (West Virginia Geological and Economic Survey 2002a). The concentrations of Zr in the 6 m seam coal is observed to be higher than that of the 18 m seam coal, which suggest the detrital origin of the coal samples and its introduction in the peat forming swamp as extremely small waterborne and windblown grains (West Virginia Geological and Economic Survey 2002b). Clay minerals observed in the SEM–EDS analysis of the coals and OB are also

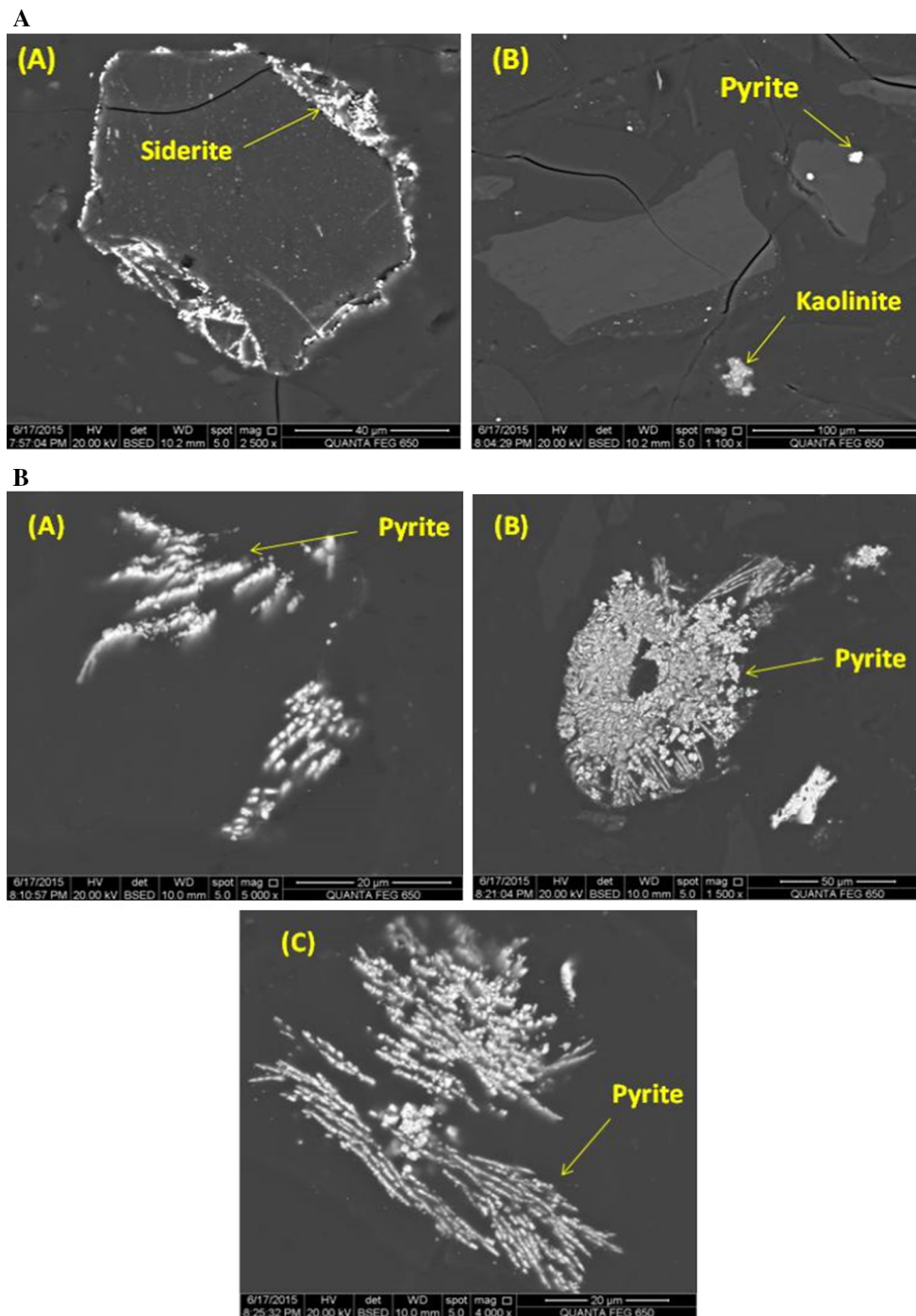


**Fig. 4** SEM-EDS images (back scattered electron) of **a** T-60F coal sample **b** T-60W sample

responsible for the presence of trace amounts of Sr, Hf, Li, V, Ga, Rb, Ba, Nb, Cs, U, Th, Zr, and the REE in these coals (Dai et al. 2014a). However, the trace elements Pb, Cd, Mo, Cu, Tl, Sn, Sb, and Zn are also found due to the presence of pyrite as these elements have a strong affinity towards pyrite (Tian et al. 2014).

In the studied OB samples, based on the whole coal basis, the concentrations of the trace elements are seen to

**Fig. 5** SEM-EDS images (back scattered electron) of **a** TO-60F **b** TO-60W samples

be more than that of the coal samples. The OB samples have high concentration of Li, V, Cr, Ni, Zn, Rb, Sr, Zr, and Ba and significant amounts of Co, Cu, Ga, As, Pb, and Nb. The lithological study of the overburden area of the Makum coalfield reveals the presence of sandstones with

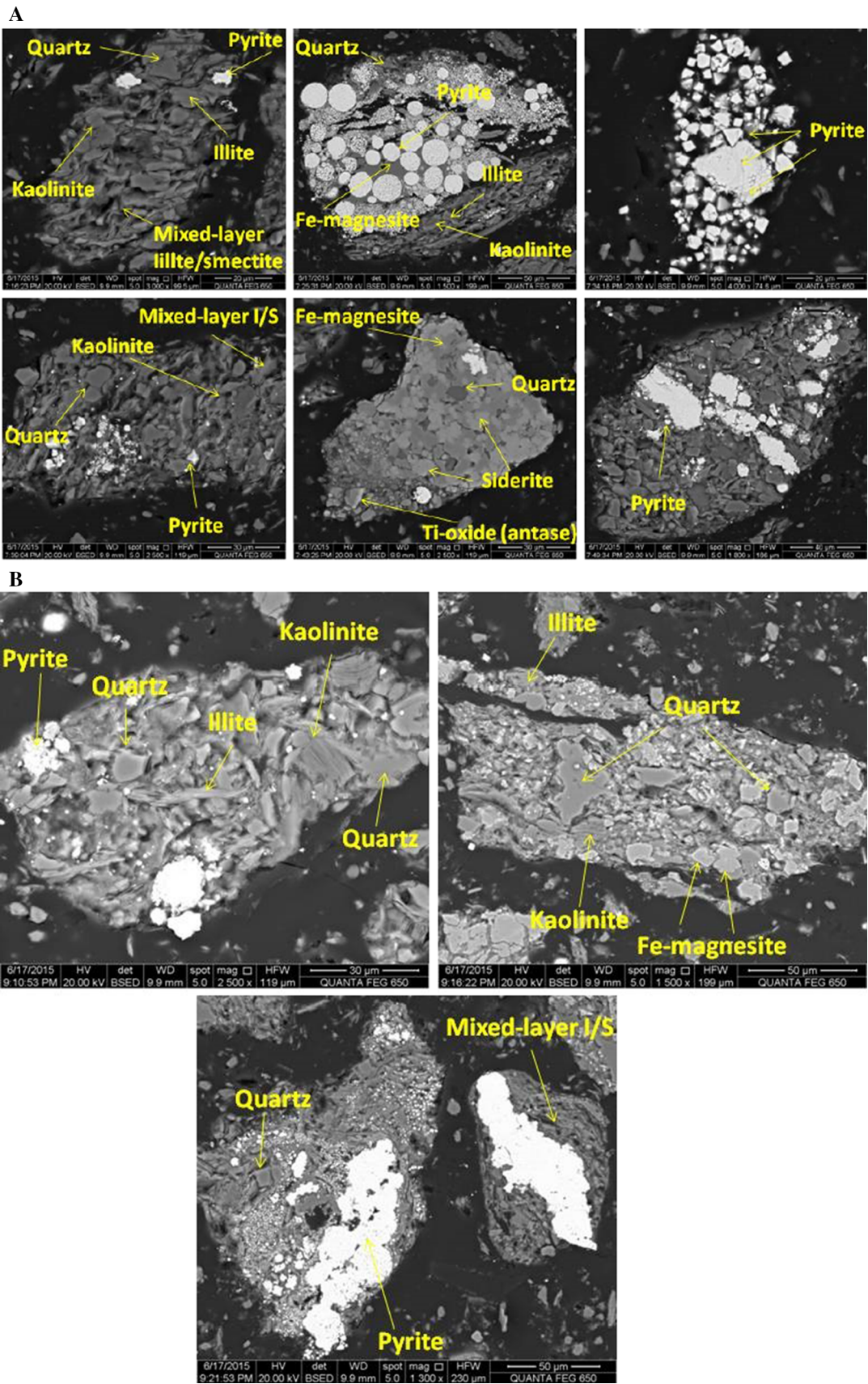


**Table 4** XRF analysis of major element oxides in the coal and OB ash samples (wt%)

| Samples                        | T-20F | T-60F | TO-20F | TO-60F |
|--------------------------------|-------|-------|--------|--------|
| LOI                            | 1.80  | 2.85  | 0.47   | 0.72   |
| SiO <sub>2</sub>               | 27.60 | 33.37 | 64.01  | 64.42  |
| TiO <sub>2</sub>               | 0.71  | 0.85  | 1.33   | 1.28   |
| Al <sub>2</sub> O <sub>3</sub> | 35.02 | 24.97 | 22.92  | 20.64  |
| Fe <sub>2</sub> O <sub>3</sub> | 8.83  | 21.90 | 6.79   | 7.89   |
| MnO                            | 0.12  | 0.13  | 0.05   | 0.09   |
| MgO                            | 4.45  | 3.42  | 0.98   | 1.36   |
| CaO                            | 3.06  | 3.29  | 0.23   | 0.38   |
| Na <sub>2</sub> O              | 8.15  | 4.29  | 0.34   | 0.41   |
| K <sub>2</sub> O               | 0.91  | 1.18  | 2.64   | 2.38   |
| P <sub>2</sub> O <sub>5</sub>  | 1.67  | 0.17  | 0.07   | 0.06   |
| SO <sub>3</sub>                | 3.31  | 2.35  | 0.17   | 0.37   |

sandy shale, clay, sandy clay, and carbonaceous shale (Sarmah 2013). The lithology indicates a possibility of occurrence of the trace and rare earth elements in the coalfield. Moreover, the groundwater in the mined areas may have lead to the mobilization and dispersion of the elements which, in turn, were deposited in the porous and permeable overburden rock units.

The water leaching experiment also indicates the leaching/removal of majority of elements from coal (T-20W, T-60W) as well as OB (TOL-20W, TO-60W) (Table 5). The concentrations of the elements in the water leachates of both coal (TL-20, TL-60) and OB (TOL-20, TOL-60, LS-60F) samples are less in comparison to their counterpart samples. Most of the trace and REEs such as V, Ga, Nb, Hf, and Zr present in the overburden samples are due to the presence of clay and shales in Makum coalfield (Assam) (Dai et al. 2012a). The Sc observed in the OB sample may be due to the deposition of soil and groundwater enriched with organic acids in the coal bearing strata (Arbuzov et al. 2014).

Trace elements are also associated with the organic matter to a greater or lesser extent (Spears 2015). Germanium, V, and Be are mainly associated with organic matter, particularly with vitrinite group macerals (Spears 2015), which are observed to be dominant in these Paleogene coals (Table 2).

The presence of some selected major, minor, and trace elements in Makum coalfield were previously reported (Saikia et al. 2009; Khare and Baruah 2010; Saikia et al. 2015). The aqueous leaching experiment shows that these trace elements, including the REEs, present within the coal and overburden samples are released (Table 5). The mobilization of these elements may be further enhanced by the acid mine drainage in the coalfield. Thus, the

concentrations of the trace elements such as As, B, Pb, and Se are of great concern; Cu and V of moderate concern; Ba, Ge, and Mn of minor concern; and Sn of less environmental concern in these coals. However, the concentrations of the elements, including REEs, are found to be less than that in the Earth's crust (Mukherjee and Srivastava 2005).

#### Distribution of rare earth elements in the coals and OB

The rare earth elements and yttrium (REY, or REE if yttrium is not included) are divided into light REE (LREE-La, Ce, Pr, Nd, and Sm), medium REE (MREE-Eu, Gd, Tb, Dy, and Y), and heavy REE (HREE-Ho, Er, Tm, Yb, and Lu) groups (Seredin and Dai 2012). Seredin and Dai (2012) devised a classification which divides REE into three groups relevant to the utilization: critical (Nd, Eu, Tb, Dy, Y, and Er), uncritical (La, Pr, Sm, and Gd), and excessive (Ce, Ho, Tm, Yb, and Lu). From Table 5, it is observed that the concentrations of LREE, MREE, and HREE in the coal samples are lower in comparison to that of the OB samples. The average REY content in both 6 and 18 m coal and their associated OB samples are found to be 0.07, 0.05, 0.98, and 2.39 ppm, respectively, which are much lower in comparison to global (68.5 ppm) (Ketris and Yudovich 2009), Chinese coals (137.9 ppm) (Dai et al. 2012c), and USA (62.1 ppm) (Finkelman 1993) coals.

The depletion in the distribution patterns of REEs in the samples from the Makum coalfield may be attributed to their marine depositional environments, differential weathering, varying thickness of the coal seams (Seredin and Dai 2012; Diehl et al. 2012), and, possibly, due to its low mineral matter (low ash yield) (Koeppenkastrup and De Carlo 1993; White 2000; Coppin et al. 2002; Saikia et al. 2014a, b). The REEs in coals may be present due to continuous dispersal of these elements from minerals such as kaolinite and illite in the source area by the intrusion of sea water during diagenesis of these coals (Singh and Singh 2002). The presence of the marine influence has been observed through the petrographical study of the coal macerals. The presence of Y, La, Ce, and Nd indicates the association with terrigenous material input (Singh and Singh 2002; Seredin and Dai 2012) and natural waters enriched in Y and REE during diagenesis of these Paleogene coals (Dai et al. 2006a, b).

The distribution of the REEs and other trace elements in coal and OBs normalized by upper continental crust (UCC) (Liu et al. 2014) are illustrated in Figs. 6 and 7, respectively. The coal and overburden samples of 6 m and 18 m seams show enrichment of light, medium, and heavy REE and have negative Tb, Ho, Tm, and Lu anomalies, as compared to the upper continental crust. However, the anomalies are seen to be more in the overburden samples

**Table 5** Concentration of trace elements (including REEs) in the coal, overburden, leached coal, leached overburden, and water leachate samples (ppm, whole-sample basis)

| Samples | OBs              |                            |                         |                  |                            |                         |               |        |             |                           |                             |             |                            |                             |        |
|---------|------------------|----------------------------|-------------------------|------------------|----------------------------|-------------------------|---------------|--------|-------------|---------------------------|-----------------------------|-------------|----------------------------|-----------------------------|--------|
|         | Coals            |                            |                         | OBs              |                            |                         |               |        |             |                           |                             |             |                            |                             |        |
|         | T-20F (raw coal) | T-20W (water leached coal) | TL-20 (water leachates) | T-60F (raw coal) | T-60W (water leached coal) | TL-60 (water leachates) | T2-60F (coal) | MK-60F | TO-20F (OB) | TO-20W (water leached OB) | TOL-20 (OB water leachates) | TO-60F (OB) | TO-60 W (water leached OB) | TOL-60 (OB water leachates) | LS-60F |
| Li      | 4.85             | 4.70                       | 2.41 × 10 <sup>-2</sup> | 3.68             | 3.37                       | 8.98 × 10 <sup>-3</sup> | 2.46          | 1.68   | 98.96       | 95.19                     | 1.18 × 10 <sup>-1</sup>     | 67.83       | 64.81                      | 6.57 × 10 <sup>-2</sup>     | 49.46  |
| Be      | 0.19             | 0.19                       | bdl                     | 0.11             | 0.10                       | 0.14 × 10 <sup>-4</sup> | 0.14          | 0.49   | 1.87        | 1.81                      | 2.26 × 10 <sup>-3</sup>     | 1.59        | 1.53                       | 0.51 × 10 <sup>-4</sup>     | 1.89   |
| Sc      | 0.85             | 0.43                       | 7.42 × 10 <sup>-3</sup> | 0.60             | 0.12                       | 5.31 × 10 <sup>-4</sup> | 0.58          | 0.85   | 18.42       | 17.23                     | 9.56 × 10 <sup>-3</sup>     | 17.95       | 18.57                      | 2.13 × 10 <sup>-3</sup>     | 17.83  |
| V       | 3.02             | 2.96                       | 0.59 × 10 <sup>-4</sup> | 4.19             | 4.42                       | 0.86 × 10 <sup>-4</sup> | 3.92          | 3.28   | 162.61      | 163.81                    | 1.11 × 10 <sup>-4</sup>     | 154.78      | 155.53                     | 1.35 × 10 <sup>-4</sup>     | 139.39 |
| Cr      | bdl              | 2.65                       | 1.42 × 10 <sup>-2</sup> | 1.78             | 11.76                      | 4.75 × 10 <sup>-3</sup> | 4.14          | 10.59  | 222.66      | 224.09                    | 2.15 × 10 <sup>-3</sup>     | 187.13      | 187.42                     | 5.13 × 10 <sup>-4</sup>     | 183.03 |
| Co      | 0.64             | 0.65                       | 2.57 × 10 <sup>-2</sup> | 0.63             | 0.69                       | 3.79 × 10 <sup>-2</sup> | 0.91          | 1.94   | 20.60       | 18.39                     | 5.61 × 10 <sup>-1</sup>     | 27.83       | 23.74                      | 1.19                        | 23.88  |
| Ni      | bdl              | 2.46                       | 0.132                   | 0.92             | 8.52                       | 1.91 × 10 <sup>-1</sup> | 6.08          | 7.73   | 129.56      | 123.42                    | bdl                         | 135.92      | 117.92                     | bdl                         | 111.41 |
| Cu      | 1.64             | 1.00                       | 1.09 × 10 <sup>-2</sup> | 3.20             | 2.72                       | 5.34 × 10 <sup>-3</sup> | 2.29          | 2.08   | 39.24       | 40.60                     | 3.87 × 10 <sup>-2</sup>     | 34.09       | 36.69                      | 4.58 × 10 <sup>-3</sup>     | 39.74  |
| Zn      | 8.27             | 15.09                      | 0.335                   | 58.43            | 30.23                      | 4.18                    | 4.65          | 8.90   | 99.39       | 104.36                    | 1.30                        | 110.23      | 126.48                     | 1.52                        | 131.74 |
| Ga      | 0.91             | 0.88                       | 0.8 × 10 <sup>-4</sup>  | 0.68             | 0.71                       | 0.19 × 10 <sup>-4</sup> | 0.56          | 0.67   | 23.11       | 22.81                     | 0.98 × 10 <sup>-4</sup>     | 21.19       | 20.37                      | 0.79 × 10 <sup>-4</sup>     | 20.03  |
| Ge      | 0.32             | Bdl                        | 3.3 × 10 <sup>-4</sup>  | 0.24             | bdl                        | 0.68 × 10 <sup>-4</sup> | 0.10          | 0.25   | 1.93        | 1.26                      | 3.42 × 10 <sup>-4</sup>     | 1.49        | 0.84                       | 0.63 × 10 <sup>-4</sup>     | 1.65   |
| As      | 0.49             | Nd                         | nd                      | 1.33             | nd                         | nd                      | 1.37          | 1.43   | 8.09        | nd                        | nd                          | 8.13        | nd                         | nd                          | 14.12  |
| Se      | 0.55             | Nd                         | nd                      | 0.52             | nd                         | nd                      | 122.48        | 62.91  | 0.39        | nd                        | nd                          | 0.25        | nd                         | nd                          | 1.14   |
| Rb      | 0.63             | 0.68                       | 3.84 × 10 <sup>-3</sup> | 1.34             | 1.31                       | 1.24 × 10 <sup>-2</sup> | 1.34          | 5.41   | 113.36      | 113.60                    | 9.73 × 10 <sup>-2</sup>     | 101.15      | 101.67                     | 7.13 × 10 <sup>-2</sup>     | 93.89  |
| Sr      | 190.26           | 220.14                     | 2.27                    | 54.21            | 49.88                      | 2.48                    | 3.84          | 2.65   | 195.01      | 247.11                    | 3.82 × 10 <sup>-1</sup>     | 145.49      | 160.49                     | 0.49                        | 121.88 |
| Y       | 2.92             | 3.09                       | 0.9 × 10 <sup>-5</sup>  | 1.16             | 0.97                       | 2.01 × 10 <sup>-4</sup> | bdl           | 0.94   | 19.40       | 19.22                     | 4.19 × 10 <sup>-3</sup>     | 18.34       | 19.92                      | 7.69 × 10 <sup>-4</sup>     | 23.06  |
| Zr      | 27.27            | 29.01                      | bdl                     | 4.72             | 5.97                       | 0.37 × 10 <sup>-4</sup> | 0.41          | 0.27   | 156.87      | 175.61                    | bdl                         | 154.81      | 171.70                     | bdl                         | 159.71 |
| Nb      | 0.60             | 0.57                       | bdl                     | 0.28             | 0.34                       | bdl                     | 0.02          | 0.02   | 14.09       | 13.92                     | bdl                         | 14.15       | 14.05                      | bdl                         | 13.07  |
| Mo      | bdl              | 0.29                       | 4.31 × 10 <sup>-4</sup> | bdl              | 1.15                       | 0.35 × 10 <sup>-4</sup> | 0.00          | 0.00   | 2.23        | 2.26                      | 0.53 × 10 <sup>-4</sup>     | 1.17        | 1.27                       | 0.28 × 10 <sup>-4</sup>     | 0.88   |
| Cd      | 0.04             | Bdl                        | 0.58 × 10 <sup>-4</sup> | 0.03             | bdl                        | 1.06 × 10 <sup>-3</sup> | 0.04          | 0.09   | 0.27        | 0.56                      | 1.79 × 10 <sup>-3</sup>     | 0.27        | 0.32                       | 1.53 × 10 <sup>-3</sup>     | 0.91   |
| In      | 0.00             | 0.00                       | 0                       | 0.00             | 0.00                       | 0                       | 0.02          | 0.04   | 0.08        | 0.09                      | 0.01 × 10 <sup>-4</sup>     | 0.07        | 0.09                       | 0                           | 0.32   |
| Sn      | 0.04             | 0.07                       | bdl                     | 0.17             | 0.18                       | bdl                     | 0.09          | 0.11   | 2.57        | 2.99                      | bdl                         | 3.44        | 5.93                       | bdl                         | 0.08   |
| Sb      | 0.05             | 0.04                       | 0.45 × 10 <sup>-4</sup> | 0.05             | 0.04                       | 0.32 × 10 <sup>-4</sup> | 113.87        | 50.37  | 0.42        | 0.37                      | 0.01 × 10 <sup>-4</sup>     | 0.29        | 0.32                       | 0.11 × 10 <sup>-4</sup>     | 2.47   |
| Cs      | 0.04             | 0.05                       | 1.31 × 10 <sup>-4</sup> | 0.12             | 0.13                       | 3.90 × 10 <sup>-4</sup> | 1.00          | 1.96   | 8.49        | 8.79                      | 1.64 × 10 <sup>-3</sup>     | 6.76        | 7.01                       | 1.27 × 10 <sup>-3</sup>     | 0.47   |
| Ba      | 59.46            | 61.58                      | 8.58 × 10 <sup>-2</sup> | 91.86            | 97.20                      | 4.95 × 10 <sup>-2</sup> | 2.34          | 3.93   | 294.09      | 311.43                    | 3.61 × 10 <sup>-2</sup>     | 344.07      | 341.53                     | 3.17 × 10 <sup>-2</sup>     | 6.53   |
| La      | 3.55             | 3.45                       | bdl                     | 1.37             | 1.18                       | 1.32 × 10 <sup>-4</sup> | 0.23          | 0.42   | 30.13       | 26.35                     | 7.11 × 10 <sup>-4</sup>     | 28.31       | 26.68                      | 1.56 × 10 <sup>-4</sup>     | 295.51 |
| Ce      | 7.18             | 7.12                       | bdl                     | 2.64             | 2.29                       | 2.23 × 10 <sup>-4</sup> | 0.98          | 2.00   | 65.29       | 57.00                     | 1.66 × 10 <sup>-3</sup>     | 62.83       | 58.47                      | 1.41 × 10 <sup>-4</sup>     | 30.77  |
| Pr      | 0.78             | 0.88                       | bdl                     | 0.31             | 0.29                       | 0.22 × 10 <sup>-4</sup> | 0.21          | 0.45   | 6.88        | 6.73                      | 2.23 × 10 <sup>-4</sup>     | 6.66        | 6.85                       | 0.12 × 10 <sup>-4</sup>     | 68.06  |
| Nd      | 3.06             | 3.43                       | bdl                     | 1.28             | 1.16                       | 0.97 × 10 <sup>-4</sup> | 0.08          | 0.15   | 27.60       | 27.04                     | 1.07 × 10 <sup>-3</sup>     | 27.19       | 27.79                      | 0.47 × 10 <sup>-4</sup>     | 7.27   |
| Sm      | 0.60             | 0.69                       | 0.02 × 10 <sup>-4</sup> | 0.27             | 0.26                       | 0.11 × 10 <sup>-4</sup> | 0.28          | 0.64   | 5.41        | 5.24                      | 3.75 × 10 <sup>-4</sup>     | 5.26        | 5.39                       | 0.08 × 10 <sup>-4</sup>     | 29.73  |
| Eu      | 0.11             | 0.13                       | 0.14 × 10 <sup>-4</sup> | 0.07             | 0.06                       | 0.12 × 10 <sup>-4</sup> | 0.03          | 0.10   | 1.20        | 1.19                      | 1.29 × 10 <sup>-4</sup>     | 1.21        | 1.20                       | 0.01 × 10 <sup>-4</sup>     | 6.00   |
| Gd      | 0.67             | 0.73                       | 0.02 × 10 <sup>-4</sup> | 0.27             | 0.28                       | 0.25 × 10 <sup>-4</sup> | 0.21          | 0.59   | 5.30        | 5.20                      | 7.25 × 10 <sup>-4</sup>     | 5.13        | 5.28                       | 0.47 × 10 <sup>-4</sup>     | 1.39   |
| Tb      | 0.08             | 0.10                       | 0                       | 0.03             | 0.03                       | 0.03 × 10 <sup>-4</sup> | 0.04          | 0.12   | 0.67        | 0.69                      | 1.36 × 10 <sup>-4</sup>     | 0.66        | 0.71                       | 0.07 × 10 <sup>-4</sup>     | 6.13   |
| Dy      | 0.54             | 0.61                       | 0                       | 0.24             | 0.21                       | 0.22 × 10 <sup>-4</sup> | 0.12          | 0.34   | 3.96        | 3.93                      | 9.11 × 10 <sup>-4</sup>     | 3.86        | 4.10                       | 0.53 × 10 <sup>-4</sup>     | 0.82   |
| Ho      | 0.10             | 0.12                       | 0                       | 0.04             | 0.04                       | 0.04 × 10 <sup>-4</sup> | 0.01          | 0.04   | 0.75        | 0.74                      | 1.45 × 10 <sup>-4</sup>     | 0.72        | 0.76                       | 0.01 × 10 <sup>-3</sup>     | 4.66   |

Table 5 continued

| Samples | Coals            |                            |                         |                  |                            |                              | OBs    |        |             |                           |                             |             | LS-60F |                            |                             |
|---------|------------------|----------------------------|-------------------------|------------------|----------------------------|------------------------------|--------|--------|-------------|---------------------------|-----------------------------|-------------|--------|----------------------------|-----------------------------|
|         | T-20F (raw coal) | T-20W (water leached coal) | TL-20 (water leachates) | T-60F (raw coal) | T-60W (water leached coal) | TL-60 (coal water leachates) | T2-60F | MK-60F | TO-20F (OB) | TO-20W (water leached OB) | TOL-20 (OB water leachates) | TO-60F (OB) |        | TO-60 W (water leached OB) | TOL-60 (OB water leachates) |
| Er      | 0.32             | 0.34                       | 0                       | 0.13             | 0.11                       | $0.12 \times 10^{-4}$        | 0.10   | 0.26   | 2.32        | 2.31                      | $3.68 \times 10^{-4}$       | 2.19        | 2.41   | $0.23 \times 10^{-4}$      | 0.88                        |
| Tm      | 0.04             | 0.05                       | 0                       | 0.02             | 0.01                       | $0.01 \times 10^{-4}$        | 0.01   | 0.03   | 0.30        | 0.31                      | $0.04 \times 10^{-3}$       | 0.30        | 0.33   | $0.02 \times 10^{-4}$      | 2.58                        |
| Yb      | 0.33             | 0.35                       | 0                       | 0.13             | 0.10                       | $0.12 \times 10^{-4}$        | 0.12   | 0.07   | 2.18        | 2.19                      | $0.25 \times 10^{-3}$       | 2.14        | 2.30   | $0.08 \times 10^{-4}$      | 0.35                        |
| Lu      | 0.05             | 0.05                       | 0                       | 0.01             | 0.01                       | $0.01 \times 10^{-4}$        | 0.01   | 0.02   | 0.30        | 0.32                      | $0.32 \times 10^{-4}$       | 0.29        | 0.32   | $0.02 \times 10^{-4}$      | 2.52                        |
| Hf      | 0.66             | 0.80                       | 0                       | 0.13             | 0.21                       | 0                            | 0.03   | 16.70  | 3.93        | 5.22                      | $0.05 \times 10^{-4}$       | 3.83        | 5.02   | 0                          | 0.35                        |
| Ta      | 0.01             | 0.01                       | bdl                     | 0.02             | 0.02                       | bdl                          | 0.02   | 0.01   | 0.97        | 1.04                      | 0                           | 0.95        | 1.03   | bdl                        | 3.81                        |
| W       | 0.11             | Bdl                        | $0.14 \times 10^{-4}$   | 0.07             | bdl                        | bdl                          | 0.70   | 0.54   | 1.39        | 2.92                      | bdl                         | 1.27        | 2.36   | bdl                        | 0.85                        |
| Tl      | 0.01             | 0.01                       | $0.08 \times 10^{-4}$   | 0.01             | 0.02                       | $0.45 \times 10^{-4}$        | 0.12   | bdl    | 0.51        | 0.48                      | $2.34 \times 10^{-4}$       | 0.45        | 0.38   | $0.85 \times 10^{-4}$      | 1.37                        |
| Pb      | 1.08             | 0.87                       | $0.05 \times 10^{-4}$   | 1.58             | 1.84                       | $8.81 \times 10^{-4}$        | bdl    | bdl    | 18.14       | 19.58                     | $9.95 \times 10^{-4}$       | 17.43       | 18.93  | bdl                        | 0.48                        |
| Bi      | 0.02             | 0.02                       | 0                       | 0.02             | 0.02                       | 0                            | 0.10   | 0.08   | 0.19        | 0.25                      | 0                           | 0.11        | 0.22   | bdl                        | 21.21                       |
| Th      | 0.30             | 0.33                       | bdl                     | 0.46             | 0.59                       | $0.01 \times 10^{-4}$        | 1.37   | 1.43   | 10.28       | 9.91                      | $0.03 \times 10^{-4}$       | 9.42        | 9.85   | bdl                        | 0.26                        |
| U       | 0.42             | 0.46                       | 0                       | 0.12             | 0.12                       | $0.12 \times 10^{-4}$        | 122.48 | 62.91  | 2.10        | 2.06                      | $1.44 \times 10^{-4}$       | 2.03        | 2.10   | 0                          | 10.84                       |

bdl below detection limit; nd: not detected

than the coal samples. The variation in the distribution of the trace elements are observed to be more in the overburden samples in comparison to that of the coal samples for both the coal seams.

**Aqueous leaching of coals and OBs and distribution of elements**

A large volume of the overburden (OB) materials generated during mining of coals in Makum coalfield (Northeast India) is exposed to the environment. The potentially hazardous elements (PHE) may be leached from coal as well as OB after contamination with ground water and during rainy season. The studied area experiences humid summer during the months of May and June with temperature rising up to 36 °C. The average humidity ranges from 87 to 91 % during the wet months. The area experiences a very high annual precipitation from 300 to 425 cm and bulk of the precipitation is in the months from April to September. Numerous rivers, streams and water channels are present in the studied area which is almost perennial due to high precipitation (CMPDI 1987).

To understand the effect of water to these materials, an aqueous leaching experiment was performed. The distribution of elements including REEs in the raw, washed (leached), and aqueous leachates are summarized in Table 5. In the leaching test, we have used deionized water, in the event that, leachates have acidic pH, which also has high ability to dissolution and leaching of elements. It is observed that the extent of leachabilities of the elements by water from coal as well as OB samples is not very significant except for a few of the elements. Scandium, Cu, and Ag are observed to be removed relatively in higher amount from the coals than the rest by aqueous leaching. In case of OB sample, Ce is leached by about 12 % after aqueous leaching, which is an interesting finding for mineral processing due to the numerous commercial applications of Ce in glass, ceramics, and catalyst for petroleum refining (Taylor and McLennan 1985). The presence of the elements in the leachates indicated their association with the mineral or inorganic phases of the coals and OB as the elements present in organic phases cannot be released easily by water (Wills 1988). The phase transformations that mineral matter in coal undergoes as well as the changes of the pH of the leachates during aqueous leaching may also enhance the removal of trace elements from the coal matrix (Baruah et al. 2003, 2006). The release of elements is reported to be increased with the increase in leaching (Baruah et al. 2003). Elements in coal and overburden are likely to be released from the storage/disposal/application site when they come in contact with water. The behavior of the elements during leaching is mainly controlled by pH and mineralogy. The pH of the

**Fig. 6** Distribution of REYs in coals and overburdens normalized by upper continental crust (UCC)

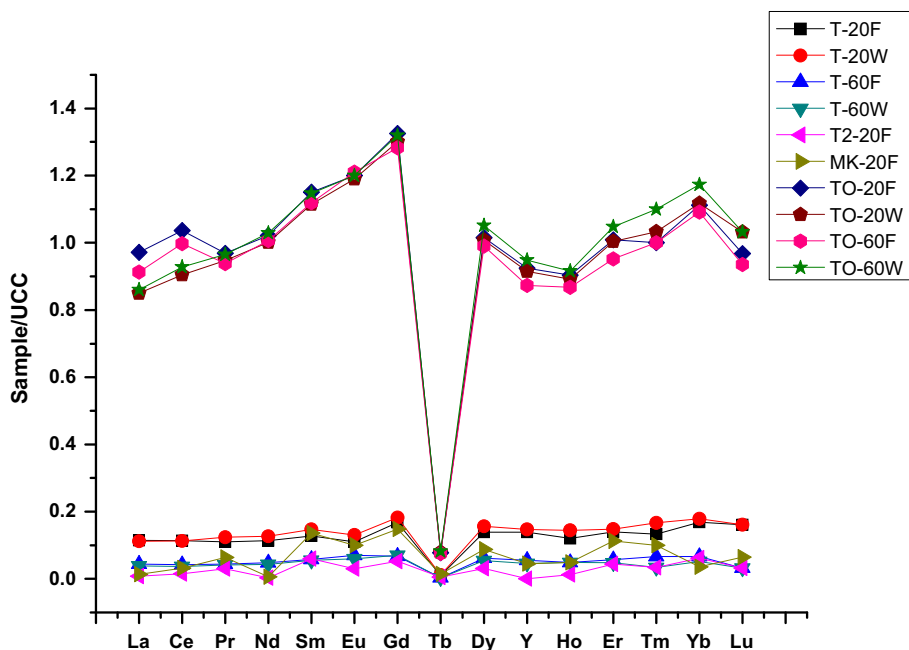
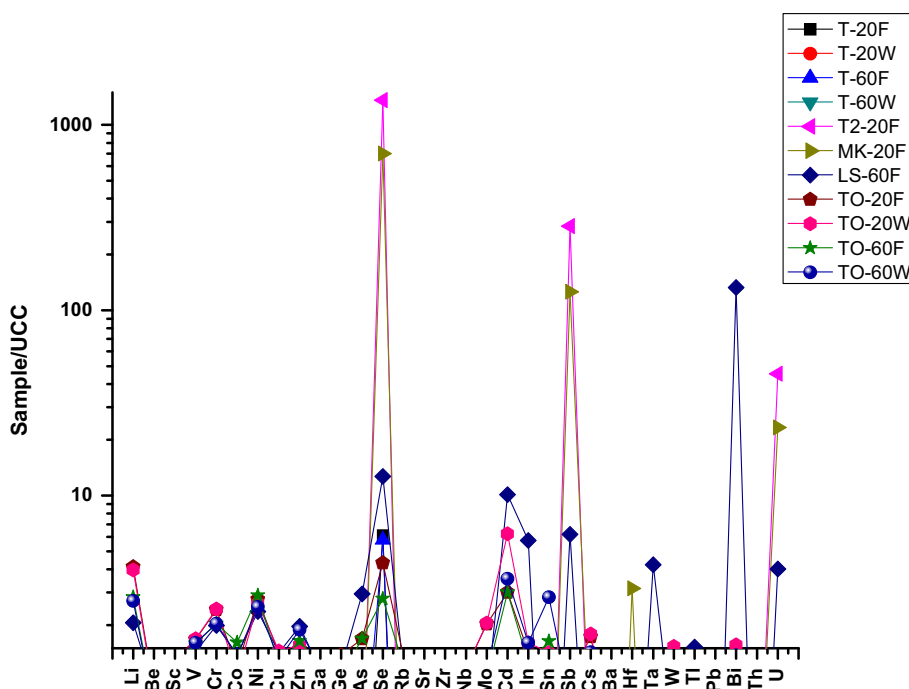


**Fig. 7** Distribution of trace elements in coals and overburdens normalized by upper continental crust (UCC)



mine water from Makum coalfield is highly acidic in nature (pH ~2.5) in comparison to other Indian mines which are near neutral to slightly alkaline leachate (Equeenuddin 2015). This is due to the leaching of pyrite, the dominant mineral found in the coals of this area. The concentrations of all the elements are high which can be attributed to the oxidation of pyrite, which increases the solubility of metals under highly acidic conditions (Jones 1995; Equeenuddin 2015).

However, the understanding of the reasons underlying the mobility of these elements is required for better control over environmental impacts in the wide variety of utilization and disposal practices. It may also assist in cost-effective design of management strategies and in the decision making of regulatory agencies. Thus, this aqueous leaching study may bring out a significant relationship in determining the association and mobilization of elements in the AMD-affected areas of coal mine.

**Table 6** Chi squared test for trace elements and REE in the coal, overburden, leached coal, leached overburden, and water leachate samples

| Samples | Mean   | Std. deviation | $\chi^2$ test |    |                |
|---------|--------|----------------|---------------|----|----------------|
|         |        |                | $\chi^2$      | df | <i>p</i> value |
| Li      | 26.48  | 37.48          | 0.00          | 14 | 1              |
| Be      | 0.66   | 0.80           | 0.87          | 13 | 0.99           |
| Sc      | 6.23   | 8.63           | 0.87          | 13 | 0.99           |
| V       | 53.19  | 74.87          | 0.00          | 14 | 1              |
| Cr      | 69.02  | 97.19          | 0.00          | 14 | 1              |
| Co      | 8.11   | 10.99          | 0.00          | 14 | 1              |
| Ni      | 42.95  | 59.35          | 3.20          | 12 | 0.99           |
| Cu      | 13.56  | 18.03          | 0.00          | 14 | 1              |
| Zn      | 47.01  | 52.01          | 0.00          | 14 | 1              |
| Ga      | 7.46   | 10.31          | 0.00          | 14 | 1              |
| Ge      | 0.54   | 0.69           | 0.87          | 13 | 0.99           |
| As      | 2.33   | 4.27           | 22.87         | 7  | 0.001          |
| Se      | 12.55  | 34.43          | 22.87         | 7  | 0.001          |
| Rb      | 35.64  | 50.79          | 0.87          | 13 | 0.99           |
| Sr      | 93.11  | 92.95          | 0.00          | 14 | 1              |
| Y       | 7.27   | 9.41           | 0.00          | 14 | 1              |
| Zr      | 59.01  | 77.31          | 3.20          | 12 | 0.99           |
| Nb      | 4.74   | 6.68           | 6.27          | 10 | 0.79           |
| Mo      | 0.62   | 0.83           | 6.60          | 11 | 0.83           |
| Cd      | 0.17   | 0.26           | 1.80          | 11 | 0.99           |
| In      | 0.05   | 0.08           | 16.47         | 7  | 0.02           |
| Sn      | 1.04   | 1.82           | 6.60          | 11 | 0.83           |
| Sb      | 11.22  | 31.19          | 1.47          | 12 | 0.99           |
| Cs      | 2.32   | 3.47           | 0.00          | 14 | 1              |
| Ba      | 107.61 | 138.89         | 0.00          | 14 | 1              |
| La      | 27.81  | 75.05          | 0.00          | 14 | 1              |
| Ce      | 19.77  | 26.83          | 0.00          | 14 | 1              |
| Pr      | 6.54   | 17.27          | 0.00          | 14 | 1              |
| Nd      | 8.40   | 12.02          | 0.00          | 14 | 1              |
| Sm      | 3.58   | 7.58           | 0.00          | 14 | 1              |
| Eu      | 0.75   | 1.54           | 0.87          | 13 | 0.99           |
| Gd      | 1.67   | 2.25           | 0.00          | 14 | 1              |
| Tb      | 0.62   | 1.55           | 0.87          | 13 | 0.99           |
| Dy      | 1.25   | 1.71           | 0.00          | 14 | 1              |
| Ho      | 0.53   | 1.18           | 3.20          | 12 | 0.996          |
| Er      | 0.76   | 0.99           | 0.00          | 14 | 1              |
| Tm      | 0.26   | 0.65           | 1.47          | 12 | 0.99           |
| Yb      | 0.68   | 0.96           | 0.87          | 13 | 0.99           |
| Lu      | 0.26   | 0.64           | 3.33          | 10 | 0.97           |
| Hf      | 2.46   | 4.41           | 3.20          | 12 | 0.99           |
| Ta      | 0.53   | 1.01           | 5.80          | 7  | 0.56           |
| W       | 0.68   | 0.93           | 10.67         | 10 | 0.38           |
| Tl      | 0.22   | 0.37           | 3.20          | 12 | 0.99           |
| Pb      | 5.33   | 8.26           | 3.20          | 12 | 0.99           |
| Bi      | 1.48   | 5.46           | 8.40          | 8  | 0.39           |

**Table 6** continued

| Samples | Mean  | Std. deviation | $\chi^2$ test |    |                |
|---------|-------|----------------|---------------|----|----------------|
|         |       |                | $\chi^2$      | df | <i>p</i> value |
| Th      | 2.95  | 4.34           | 0.87          | 13 | 0.99           |
| U       | 13.71 | 34.09          | 0.00          | 14 | 1              |

(a) 15 cells (100.0 %) have expected frequencies less than 5. The minimum expected cell frequency is 1.0

(b) 14 cells (100.0 %) have expected frequencies less than 5. The minimum expected cell frequency is 1.1

(c) 13 cells (100.0 %) have expected frequencies less than 5. The minimum expected cell frequency is 1.2

(d) 8 cells (100.0 %) have expected frequencies less than 5. The minimum expected cell frequency is 1.9

(e) 11 cells (100.0 %) have expected frequencies less than 5. The minimum expected cell frequency is 1.4

(f) 12 cells (100.0 %) have expected frequencies less than 5. The minimum expected cell frequency is 1.3

(g) 9 cells (100.0 %) have expected frequencies less than 5. The minimum expected cell frequency is 1.7

### Statistical analysis

#### Statistical significance test

The Chi squared ( $\chi^2$ ) test was performed to test whether the distribution of the trace and REEs approximates the assumed theoretical distribution (see Table 6). It also tests whether or not a statistically significant relationship exists among the trace and REEs (IDRE 2015). The *p* value in most of the elements is greater than 0.05, indicating that these elements are present independently in the coal samples.

#### Bivariate and hierarchical cluster analyses

Bivariate analysis aids in identifying the association between variables. A probability value of  $p = 0.05$  is considered as statistically significant in this study. The correlation coefficient matrix indicates the interrelation among the elements present in the studied coal, OB, and water leachate samples. The Pearson correlation coefficients for the elements are listed (in see supplementary data) with coefficient values  $>\pm 0.5$ . The bivariate analysis showed higher values of correlation coefficients among the trace and RE elements present in coal, OB, and water samples (see supplementary data). This indicates that a strong association exists among these elements. The bivariate analysis can be further established through hierarchical clustering where pairwise similar groups of the trace and RE elements are formed (Fig. 8), and thus, are useful in deducing the elemental associations and the mode of occurrence in the coal samples. For instance, the



**Fig. 8** Hierarchical clustering analysis (HCA) of trace and REEs in the coal, OB, and water leachate samples

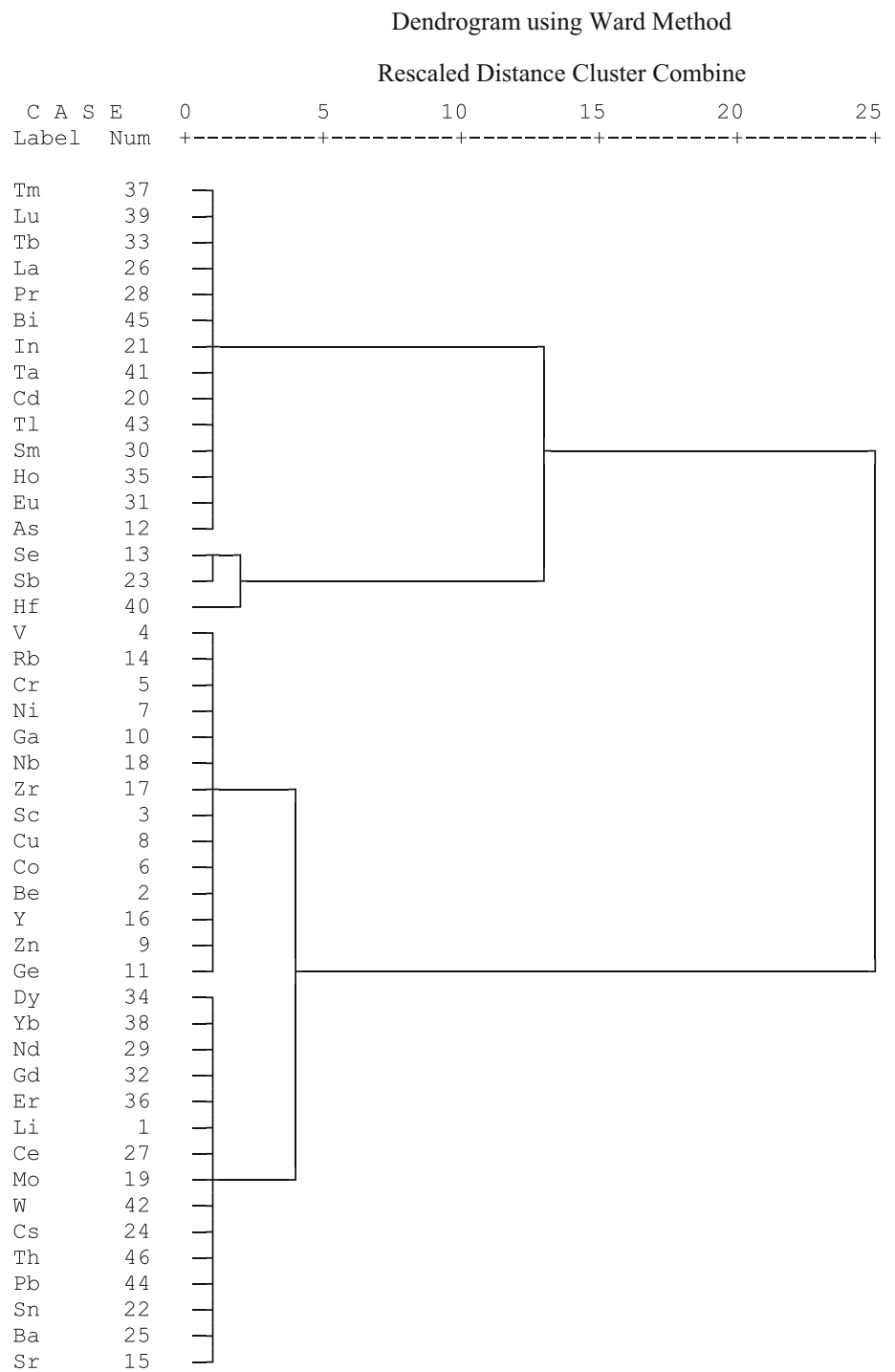


**Table 7** Eigenvalues and % variability by principal components

|              | F1    | F2     | F3    | F4    | F5    | F6    | F7    | F8    | F9    | F10   |
|--------------|-------|--------|-------|-------|-------|-------|-------|-------|-------|-------|
| Eigen value  | 30.92 | 10.491 | 3.147 | 0.783 | 0.579 | 0.522 | 0.330 | 0.125 | 0.066 | 0.028 |
| % Variance   | 65.79 | 22.32  | 6.69  | 1.67  | 1.23  | 1.11  | 0.70  | 0.27  | 0.14  | 0.06  |
| Cumulative % | 65.79 | 88.12  | 94.81 | 96.48 | 97.71 | 98.82 | 99.52 | 99.79 | 99.93 | 99.99 |

elements showing strong correlation in the bivariate analysis form homogeneous associations in the HCA.

#### Principal component analysis (PCA) of the elements

Principal component analysis (PCA) of trace elements including REEs of raw and leached coal, raw and leached OB, and water leachate samples was studied for reducing the dimensionality of the highly complex datasets, thus providing a new set of orthogonal variables and establishing a linkage between the generated datasets (Khare et al. 2011). Eliminating the components with an eigenvalue of <1, the first three components are extracted and the other components are eliminated (Table 7). When the percentages of the total variances of the three extracted components are accumulated, it can be seen that these three principal components account for 94.81 % of the total variance of the original data. Variables having loadings of >0.5 are only considered to explain each factor (see the bold values in Table 8).

F1, describing 65.79 % of the total variance of the data is highly loaded with Li, Be, Sc, V, Cr, Co, Ni, Cu, Zn, Ga, Ge, As, Rb, Sr, Y, Zr, Nb, Mo, Cd, In, Sn, Cs, Ba, La, Ce, Pr, Nd, Eu, Gd, Tb, Dy, Ho, Er, Tm, Yb, Lu, Sm, Ta, W, Tl, Pb, and Th. Yttrium is mainly associated with terrigenous materials input and natural waters enriched in yttrium. The high loadings of Y indicate that the other elements are generally concentrated in the terrigenous materials along with the Y-enriched natural waters present in the coal bearing areas (Dai et al. 2014b). The high loadings of Cu suggest that the other trace and RE elements are concentrated in chalcopyrites containing Cu (Schatzel and Stewart 2009). These elements in turn have concentrated in the leached samples of coal, OB, and water leachate samples due to acidic drainages resulting in the mobilization and retention of the trace, and RE elements in the terrigenous materials and modified kaolinite minerals of the study area (Liang et al. 2014). The presence of REE indicates that the pH of the environment is low, thus enhancing desorption of REEs and further resulting in the increase of the mobility of these elements (Xu et al. 2003). Antimony, Cd, Co, Ga, Ge, In, and Sn are located primarily in the sulfide groups present in coals (Xu et al. 2003; Dai et al. 2006a, b). The higher values of these elements indicate the association of the other elements with the sulfide groups particularly with pyrite (Spears 2015). Spears (2015) found V and Ge along with the other trace and REE elements to be associated with the vitrinite group of macerals. The significant loading of Nb and Ta suggest that the trace and REEs are associated with the clay minerals found in the coal and OB samples of the Makum coalfield since clay can be a significant source of Nb and Ta (Dai et al. 2010).

**Table 8** Matrix of the first three principal components of the trace and REEs

|    | Component   |              |             |
|----|-------------|--------------|-------------|
|    | 1           | 2            | 3           |
| Li | <b>.945</b> | -.263        | .012        |
| Be | <b>.991</b> | -.005        | .087        |
| Sc | <b>.995</b> | -.065        | .024        |
| V  | <b>.990</b> | -.123        | .017        |
| Cr | <b>.989</b> | -.115        | .025        |
| Co | <b>.975</b> | -.027        | .028        |
| Ni | <b>.987</b> | -.118        | .037        |
| Cu | <b>.997</b> | -.035        | .029        |
| Zn | <b>.959</b> | .033         | -.051       |
| Ga | <b>.993</b> | -.102        | .015        |
| G  | <b>.949</b> | .045         | .042        |
| As | <b>.672</b> | <b>.548</b>  | .075        |
| Se | -.265       | .042         | <b>.953</b> |
| Rb | <b>.989</b> | -.123        | .025        |
| Sr | <b>.670</b> | -.240        | -.234       |
| Y  | <b>.997</b> | .032         | -.020       |
| Zr | <b>.992</b> | -.082        | -.029       |
| Nb | <b>.993</b> | -.095        | -.002       |
| Mo | <b>.839</b> | -.310        | -.063       |
| Cd | <b>.859</b> | .444         | .064        |
| In | <b>.763</b> | <b>.630</b>  | .103        |
| Sn | <b>.747</b> | <b>-.536</b> | .025        |
| Sb | -.252       | .052         | <b>.946</b> |
| Cs | <b>.811</b> | <b>-.552</b> | .144        |
| Ba | <b>.773</b> | <b>-.599</b> | -.074       |
| La | <b>.575</b> | <b>.817</b>  | -.016       |
| Ce | <b>.940</b> | -.325        | -.004       |
| Pr | <b>.582</b> | <b>.812</b>  | -.012       |
| Nd | <b>.887</b> | -.457        | -.016       |
| Sm | <b>.686</b> | <b>.726</b>  | -.002       |
| Eu | <b>.713</b> | <b>.700</b>  | -.007       |
| Gd | <b>.884</b> | -.464        | .028        |
| Tb | <b>.596</b> | <b>.801</b>  | -.003       |
| Dy | <b>.866</b> | -.496        | .013        |
| Ho | <b>.662</b> | <b>.748</b>  | -.015       |
| Er | <b>.913</b> | -.404        | .027        |
| Tm | <b>.609</b> | <b>.791</b>  | -.010       |
| Yb | <b>.851</b> | <b>-.519</b> | .008        |
| Lu | <b>.612</b> | <b>.789</b>  | -.012       |
| Hf | .207        | -.251        | .470        |
| Ta | <b>.786</b> | <b>.616</b>  | -.003       |
| W  | <b>.828</b> | -.354        | .238        |
| Tl | <b>.840</b> | .535         | .055        |
| Pb | <b>.816</b> | <b>-.575</b> | -.010       |
| Bi | .447        | <b>.893</b>  | -.009       |
| Th | <b>.807</b> | <b>-.577</b> | .106        |
| U  | -.215       | .094         | <b>.962</b> |

F2, describing 22.32 % of the total variance of the data, is highly loaded with As, In, La, Pr, Sm, Eu, Tb, Ho, Tm, Lu, Ta, and Bi (positively) and Sn, Cs, Ba, Yb, Th, and Pb (negatively). The Bi is present as sulfides or associated with other sulfides in the coals. The positive and negative values of the other elements with Bi indicate their association with the sulfide groups present in the studied coal samples.

F3, describing 3.15 % of the total variance of the data, is highly loaded with Se, Sb and U. The high loading of U indicates that Se and Sb are mainly associated with monazite and clay minerals present in the studied area.

## Conclusions

The coals and associated mine overburden from Makum coalfield (Assam, India) are medium to high sulfur in nature with high organic sulfur contents (>75 % of the total S). The coals as well as the coal mine overburden are dominated by vitrinite group macerals. The mineralogical study of these Makum coals and associated coal mine overburden identified the presence of minerals such as kaolinite, pyrite, quartz, illite, dawsonite, dolomite, albite, diaspore, marcasite, gypsum, berzeliite (garnet), calcite, rutile, anatase, thenardite, mixed-layer illite/smectite, xenotime, siderite, Ti-oxide (anatase or rutile), and Fe-bearing gahnite with variations with respect to their seam depth. Pyrite is the major inorganic sulfide mineral found in Makum coals and overburden samples with tiny grains in vitrinite. Berzeliite, from garnet structural group, is reported for the first time in any Indian Paleogene coals. Pyrite in both the coals and leached coal samples are observed to be present as agglomerate and elongate in shape. The concentrations of the REEs and trace elements of coal, OB, and water leachate samples show significant variations with their depth. The coal samples have high concentrations of Sr, Zr, Ba, Li, V, and Zn. The OB samples have high concentration of Li, V, Cr, Ni, Zn, Rb, Sr, Zr, and Ba than those of Co, Cu, Ga, As, Pb, and Nb. The average REY contents (whole coal basis) in the coals (6 and 18 m seam) and OB samples (6 and 18 m seam) are found to be 1.35, 0.53, 11.45, and 11.01 ppm, respectively, which are low in comparison to world, Chinese and USA averages. The statistical analysis on the elements indicates that the association of the trace and RE elements with the mineral groups present in the coals and also their significant mutual relationships.

**Acknowledgments** The financial support from CSIR, New Delhi is thankfully acknowledged (MLP-6000-WP-III). Authors are grateful to Prof. Shifeng Dai for the analytical assistance including ICPMS, LTA-XRD, and SEM-EDS, which were supported by National Key Basic Research Program of China (No. 2014CB238902). We are

thankful to Dr James C Hower and Ms Madison Hood for petrographic data of the samples. Authors express thanks to the staff of Northeastern coalfield (Margherita) for their help in sampling. The authors are also thankful to the Director, CSIR-NEIST for his keen interest to this collaborative work. Authors are thankful to three anonymous reviewers for their constructive comments to improve the revised manuscript.

## References

- Arbuzov SI, Volostnov AV, Mezhibor A, Rybalko VI, Ilenok SS (2014) Scandium (Sc) geochemistry of coals (Siberia, Russian Far East, Mongolia, Kazakhstan, and Iran). *Int J Coal Geol* 125:22–35
- ASTM (1991) Coal and coke: standard practice for ultimate analysis of coal and coke. In: 1991 ASTM annual book of standards. ASTM International, West Conshohocken, PA 05.05
- ASTM (2002) Annual book of ASTM standard D3177-02. Test methods for total sulfur in the analysis sample of coal and coke. In: 2002 ASTM annual book of standards. ASTM International, West Conshohocken, PA (**reapproved 2007**)
- ASTM (2005) Coal and coke. Standard test method for forms of sulfur in coal. In: 2005 ASTM annual book of standards. ASTM International, West Conshohocken, PA 05.06
- ASTM (2011a) Annual book of ASTM Standard D2234/D2234M. Standard practice for collection of a gross sample of coal. In: 2010 ASTM annual book of standards. ASTM International, West Conshohocken, PA
- ASTM (2011b) Annual book of ASTM standard D3173-11. Test method for moisture in the analysis sample of coal and coke. In: 2011 ASTM annual book of standards. ASTM International, West Conshohocken, PA
- ASTM (2011c) Annual book of ASTM standard D3174-11. Test method for ash in the analysis sample of coal and coke. In: 2011 ASTM annual book of standards. ASTM International, West Conshohocken, PA
- ASTM (2011d) Annual book of ASTM standard D3175-11. Test method for volatile matter in the analysis sample of coal and coke. In: 2011 ASTM annual book of standards. ASTM International, West Conshohocken, PA
- ASTM (2011e) Annual book of ASTM standards D2798-11a. Standard test method for microscopical determination of the vitrinite reflectance of coal
- Banerjee NN, Ghosh B, Das A (2002) Trace metals in Indian coals. Allied Publishers Limited, New Delhi, pp 3–5
- Barooah PK, Baruah MK (1996) Sulphur in Assam coal. *Fuel Process Technol* 46:83–97
- Baruah BP (2009) Environmental studies around Makum coalfield, Assam, India. LAP Lambert Academic Publishing AG Co. KG, Saarbrücken, pp 16–18
- Baruah MK, Kotoky P, Baruah GC (2003) Distribution and nature of organic/mineral bound elements in Assam coals. *Fuel* 82:1783–1791
- Baruah BP, Saikia BK, Kotoky P, Rao PG (2006) Aqueous leaching on high sulfur sub-bituminous coals, in Assam, India. *Energy Fuel* 20:1550–1555
- Baruah BP, Sharma A, Saikia BK (2013) Petro-chemical investigation of some perhydrous Indian coals. *J Geol Soc India* 81:713–718
- Central Statistics Office (2015) National Statistical Organisation, Ministry of Statistics and Programme Implementation, Government of India. *Energy Stat* 22:6
- Chou C-L (2012) Sulfur in coals: a review of geochemistry and origins. *Int J Coal Geol* 100:1–13
- CMPDI (1987) Compendium on the coal occurrence of North Eastern region. A report prepared by the North Eastern Council, Ministry of Home Affairs, Government of India, II

- Coppin F, Berger G, Bauer A, Castet S, Loubet M (2002) Sorption of lanthanides on smectite and kaolinite. *Chem Geol* 182:57–68
- Dai S, Ren D, Chou C-L, Li S, Jiang Y (2006a) Mineralogy and geochemistry of the No. 6 coal (Pennsylvanian) in the Junger Coalfield, Ordos Basin, China. *Int J Coal Geol* 66:253–270
- Dai S, Zeng R, Sun Y (2006b) Enrichment of arsenic, antimony, mercury, and thallium in a late Permian anthracite from Xingren, Guizhou, Southwest China. *Int J Coal Geol* 66:217–226
- Dai S, Ren D, Zhou Y, Chou C-L, Wang X, Zhao L, Zhu X (2008) Mineralogy and geochemistry of a superhigh-organic-sulfur coal, Yanshan Coalfield, Yunnan, China: evidence for a volcanic ash component and influence by submarine exhalation. *Chem Geol* 255:182–194
- Dai S, Zhou Y, Zhang M, Wang X, Wang J, Song X, Jiang Y, Luo Y, Song Z, Yang Z, Ren D (2010) A new type of Nb (Ta)–Zr(Hf)–REE–Ga polymetallic deposit in the late Permian coal-bearing strata, eastern Yunnan, southwestern China: possible economic significance and genetic implications. *Int J Coal Geol* 83:55–63
- Dai S, Wang X, Zhou Y, Hower JC, Li D, Chen W, Zhu X (2011) Chemical and mineralogical compositions of silicic, mafic, and alkali tonsteins in the late Permian coals from the Songzao Coalfield, Chongqing, Southwest China. *Chem Geol* 282:29–44
- Dai S, Zou J, Jiang Y, Ward CR, Wang X, Li T, Liu S, Tian H, Sun X, Zhou D, Xue W (2012a) Mineralogical and geochemical compositions of the Pennsylvanian coal in the Adaohai Mine, Daqingshan Coalfield, Inner Mongolia, China: modes of occurrence and origin of diaspore, gorceixite, and ammonian illite. *Int J Coal Geol* 94:250–270
- Dai S, Jiang Y, Ward CR, Gu L, Seredin VV, Liu H, Zhou D, Wang X, Sun Y, Zou J, Ren D (2012b) Mineralogical and geochemical compositions of the coal in the Guanbanwusu Mine, Inner Mongolia, China: further evidence for the existence of an Al (Ga and REE) ore deposit in the Jungar Coalfield. *Int J Coal Geol* 98:10–40
- Dai S, Ren D, Chou C-L, Finkelman RB, Seredin VV, Zhou Y (2012c) Geochemistry of trace elements in Chinese coals: a review of abundances, genetic types, impacts on human health, and industrial utilization. *Int J Coal Geol* 94:3–21
- Dai S, Zhang W, Seredin VV, Ward CR, Hower JC, Wang X, Li X, Zhao L, Kang H, Zheng L, Wang P, Zhou D (2013) Factors controlling geochemical and mineralogical compositions of coals preserved within marine carbonate successions: a case study from the Heshan Coalfield, southern China. *Int J Coal Geol* 109–110:77–100
- Dai S, Luo Y, Seredin VV, Ward CR, Hower JC, Zhao L, Liu S, Tian H, Zou J (2014a) Revisiting the late Permian coal from the Huayingshan, Sichuan, southwestern China: enrichment and occurrence modes of minerals and trace elements. *Int J Coal Geol* 122:110–128
- Dai S, Li T, Seredin VV, Ward CR, Hower JC, Zhou Y, Zhang M, Song X, Song W, Zhao C (2014b) Origin of minerals and elements in the late Permian coals, tonsteins, and host rocks of the Xinde Mine, Xuanwei, eastern Yunnan, China. *Int J Coal Geol* 121:53–78
- Diehl SF, Goldhaber MB, Koenig AE, Lowers HA, Ruppert LF (2012) Distribution of arsenic, selenium, and other trace elements in high pyrite Appalachian coals: evidence for multiple episodes of pyrite formation. *Int J Coal Geol* 94:238–249
- Diessel CFK (2012) Coal-bearing depositional systems. Springer, Berlin, Heidelberg. doi:10.1007/978-3-642-75668-9
- Eqeenuddin SM (2015) Leaching of trace elements from Indian coal. *J Geol Soc India* 86:106–120
- Finkelman RB (1993) Trace and minor elements in coal. In: Engel MH, Macko SA (eds) Organic geochemistry. Plenum, New York, pp 593–607
- Geological Survey of India (GSI) (2009) Geology and mineral resources of Assam. Miscellaneous Publication No. 30, Part IV, Vol 2
- Institute for Digital Research and Education (IDRE) (2015) Accessed from <http://www.ats.ucla.edu/stat/spss/whatstat/whatstat.htm>
- International Committee for Coal and Organic Petrology (ICCP) (1998) The new vitrinite classification (ICCP System 1994). *Fuel* 77:349–358
- International Committee for Coal and Organic Petrology (ICCP) (2001) New inertinite classification (ICCP system 1994). *Fuel* 80:459–471
- Jamal A, Dhar BB, Ratan S (1991) Acid mine drainage in an opencast coal mine. *Mine Water Environ* 10:1–16
- Jones DR (1995) The leaching of major and trace elements from coal ash. In: Swaine DJ, Goodarzi F (eds) Environmental aspects of trace elements in coal. Kluwer Academic Publishers, Dordrecht
- Karmakar B, Ghosh T, Ojha K, Pathak AK, Devraju J (2013) Effects of chemical composition and petrography of coal for coalbed methane evaluation with special reference to in situ gas content. 10th biennial international conference and exposition, Kochi, pp 1–5
- Ketris MP, Yudovich YE (2009) Estimations of Clarkes for carbonaceous biolithes: world average for trace element contents in black shales and coals. *Int J Coal Geol* 78:135–148
- Khare P, Baruah BP (2010) Chemometric analysis of trace element distribution in raw and thermally treated high sulphur coals. *Fuel Process Technol* 91:1691–1701
- Khare P, Baruah BP, Rao PG (2011) Application of chemometrics to study the kinetics of coal pyrolysis: a novel approach. *Fuel* 90:3299–3305
- Koepfenkastrof D, De Carlo EH (1993) Uptake of rare earth elements from solution by metal oxides. *Environ Sci Technol* 27:1796–1802
- Komorek J, Rafał M (2002) Relationship between the maximum and the random reflectance of vitrinite for coal from the Upper Silesian Coal Basin (Poland). *Fuel* 81:969–971
- Li X, Dai S, Zhang W, Li T, Zheng X, Chen W (2014) Determination of As and Se in coal and coal combustion products using closed vessel microwave digestion and collision/reaction cell technology (CCT) of inductively coupled plasma mass spectrometry (ICP-MS). *Int J Coal Geol* 124:1–4
- Liang T, Li K, Wang L (2014) State of rare earth elements in different environmental components in mining areas of China. *Environ Monit Assess* 186:1499–1513
- Liu J, Jiang Y, Xie P, Li Q (2014) Geochemistry of rare earth elements and yttrium in a Ge-poor coal from the Wulantuga ore deposit, Inner Mongolia, North China. *Int J Coal Sci Technol* 1:390–394
- Loughnan FC, Goldbery R (1972) Dawsonite and Analcite in the Singleton coal measures of the Sydney Basin. *Am Miner* 57:1437–1447
- Masalehdani MNN, Mees F, Dubois M, Coquinot Y, Potdevin JL, Fialin M, Blanc-Valleron MM (2009) Condensate minerals from a burning coal-waste heap in Avion, Northern France. *Can Miner* 47:865–884
- Mishra HK, Maitra J, Sharan PK, Imam Z, Nath S (2005) Petrography of some Singrauli coals: implications for its utilisation potentiality. In: Singh AK, Sen K, Sinha A, Hazra SK (eds) International seminar on coal science and technology, pp 449–462
- Mukherjee S, Srivastava SK (2005) Trace elements in high-sulfur assam coals from the Makum Coalfield in the Northeastern region of India. *Energ Fuel* 19:882–891
- Nath S, Roy PK, Sharan PK (2005) Mineralogical study of coal by X-ray diffraction technique. In: Singh AK, Sen K, Sinha A, Hazra SK (eds) Seminar on coal science and technology, pp 473–479

- Nayak B (2013) Mineral matter and the nature of pyrite in some high sulphur tertiary coals of Meghalaya, northeast India. *J Geol Soc India* 81:203–214
- Norrish K, Hutton JT (1969) An accurate X-ray spectrographic method for the analysis of a wide range of geological samples. *Geochim Cosmochim Acta* 33(4):431–453
- Potter J, McIlreath I, Natras T (2008) Applications in CBM exploration, depositional environments and tectonic history studies geoconvention, AAPG Search and Discovery Article
- Rietveld HM (1969) A profile refinement method for nuclear and magnetic structures. *J Appl Crystallogr* 2:65–71
- Ruan CD, Ward CR (2002) Quantitative X-ray powder diffraction analysis of clay minerals in Australian coals using Rietveld methods. *Appl Clay Sci* 21:227–240
- Saikia BK, Goswamee RL, Baruah BP, Baruah RK (2009) Occurrence of some hazardous metals in Indian coals. *Coke Chem* 52(2):54–59
- Saikia BK, Dutta AM, Baruah BP (2014a) Feasibility studies of desulfurization and de-ashing of low grade medium to high sulfur coals by low energy ultrasonication. *Fuel* 123:12–18
- Saikia BK, Ward CR, Oliveira MLS, Hower JC, Baruah BP, Braga M, Silva LF (2014b) Geochemistry and nano-mineralogy of two medium-sulfur northeast Indian coals. *Int Coal Geol* 121:26–34
- Saikia BK, Wang P, Saikia A, Gupta UN, Song H, Liu J, Wei J (2015) Mineralogical and elemental composition of some high sulfur Indian tertiary coals: statistical analysis of the oxides and elements. *Energ Fuel* 29:1407–1420
- Sarmah RK (2013) Study of the maceral composition and coal facies of the oligocene coals in Makum coalfield, Upper Assam, India. *Indian J Appl Res* 3(6):281–285
- Schatzel SJ, Stewart BW (2009) A provenance study of mineral matter in coal from Appalachian Basin coal mining regions and implications regarding the respirable health of underground coal workers: a geochemical and Nd isotope investigation. *Int J Coal Geol* 94:123–136
- Senapaty A, Behera P (2015) Stratigraphic control of petrography and chemical composition of the lower Gondwana coals, Ib-valley coalfield, Odisha, India. *J Geosci Environ Prot* 3:56–66
- Seredin VV, Dai S (2012) Coal deposits as potential alternative sources for lanthanides and yttrium. *Int J Coal Geol* 94:67–93
- Singh MP, Singh AK (2002) Petrographic characteristics and depositional conditions of Eocene coals of Platform basins, Meghalaya, India. *Int J Coal Geol* 42:315–356
- Solaymani Z, Taghipour N (2012) Petrographic characteristics and palaeoenvironmental setting of Upper Triassic Olang coal deposits in northeastern Iran. *Int J Coal Geol* 92:82–89
- Spears DA (2015) The geochemistry and mineralogy of high-S coals, with examples mainly from the East Pennines Coalfield in Yorkshire and Nottinghamshire, UK: an overview. *Proc Yorks Geol Soc* 60:204–226
- Suárez-Ruiz I, Ward CR (2008) Basic factors controlling coal quality and technological behaviour of coal. In: Suárez-Ruiz I, Crelling JC (eds) *Applied coal petrology: the role of petrology in coal utilization*. Academic Press, London, pp 19–60
- Suwarno N (2006) Permian Mengkarang coal facies and environment, based on organic petrology study. *Indones J Geosci* 1(1):1–8
- Taylor JC (1991) Computer programs for standardless quantitative analysis of minerals using the full powder diffraction profile. *Powder Diffr* 6:2–9
- Taylor SR, McLennan SM (1985) *The continental crust: its composition and evolution*. Blackwell, London, p 312
- Taylor GH, Teichmüller M, Davis A, Diessel CFK, Littke R, Robert P (1998) *Organic petrology*. Gebrüder Borntraeger, Berlin, p 704
- Tian C, Zhang J, Zhao Y, Gupta R (2014) Understanding of mineralogy and residence of trace elements in coals via a novel method combining low temperature ashing and float-sink technique. *Int J Coal Geol* 131:162–171
- Ward CR (2002) Analysis and significance of mineral matter in coal seams. *Int J Coal Geol* 50:135–168
- Ward CR, Spears DA, Booth CA, Staton I, Gurba LW (1999) Mineral matter and trace elements in coals of the Gunnedah Basin, New South Wales, Australia. *Int J Coal Geol* 40:281–308
- Ward CR, Matulis CE, Taylor JC, Dale LS (2001) Quantification of mineral matter in the Argonne Premium Coals using interactive Rietveld-based X-ray diffraction. *Int J Coal Geol* 46:67–82
- West Virginia Geological and Economic Survey (2002a) Trace elements in West Virginia Coals, Strontium (Sr). <http://www.wvgs.wvnet.edu/www/datastat/te/SrHome.htm>. Accessed on 19 Oct 2015
- West Virginia Geological and Economic Survey (2002b) Trace elements in West Virginia Coals, Zirconium (Zr). <http://www.wvgs.wvnet.edu/www/datastat/te/ZrHome.htm>. Accessed on 19 Oct 2015
- White RA (2000) Behaviour of the rare earth elements in ochreous mine drainage: a laboratory and field study. PhD thesis, University of Wales, Aberystwyth
- Wills BA (1988) *Mineral processing technology: an introduction to the practical aspects of ore treatment and mineral recovery (In SI/Metric Units)*. International series on materials and technology, 4th edn. Pergamon Press, England
- Xu M, Yan R, Zheng C, Qiao Y, Han J, Sheng C (2003) Status of trace element emission in a coal combustion process: a review. *Fuel Process Technol* 85:215–237